SEMMELWEIS EGYETEM

DOKTORI ISKOLA

Ph.D. értekezések

3054.

GIUNASHVILI NINO

Kórélettan és transzlációs medicina
című program

Programvezető: Dr. Benyó Zoltán, egyetemi tanár

Témavezető: Dr. Hamar Peter, egyetemi tanár

SYNERGISTIC EFFECTS OF MODULATED ELECTRO-HYPERTHERMIA AND COX-2 INHIBITION IN TRIPLE-NEGATIVE BREAST CANCER AND MELANOMA MOUSE MODELS

PhD thesis

Nino Giunashvili, MD

Semmelweis University Doctoral School

Theoretical and Translational Medicine Division

Supervisor: Péter Hamar, MD, D.Sc

Official reviewers: Gyöngyvér Szentmártoni, MD, PhD

Oláh-Német Orsolya, MD, PhD

Head of the Complex Examination Committee: Péter Sótonyi, PhD

Members of the Complex Examination Committee: Charaf Hassan, D.Sc

Tamás Radovits, MD, PhD

Budapest

2024

Table of Contents

1. Abbreviations

5-FU: 5-fluorouracil

AA: arachidonic acid

Bcl-2: B-cell lymphoma 2

cC3: cleaved caspase 3

COX: cyclooxygenase

DAVID: the database for annotation, visualization, and integrated discovery

DEG: differential expression of genes

DNA: deoxyribonucleic acid

ER: estrogen receptors

FBS: fetal bovine serum

GO: gene ontology

gp: glycoprotein

H&E: hematoxylin and eosin

HER2: human epidermal growth factor receptor 2

ICAM: intercellular adhesion molecule

IFN-α: interferon-alpha

IHC: immunohistochemistry

IL-1β: interleukin- 1 betta

IL-6: interleukin-6

JAK: janus kinase

MAPK: mitogen-activated protein kinase

MDSC: myeloid-derived suppressor cells

mEHT: modulated electro-hyperthermia

MMP: matrix metalloproteinases

mTOR: mammalian target of rapamycin

NF-κB: nuclear factor kappa B

NK: natural killer

NSAIDs: non-steroid anti-inflammatory drugs

OR: overall response

PDK-1/Akt: phosphoinositide-dependent kinase-1/ protein kinase B

PG: prostaglandin

PR: partial response

PR: progesterone receptor

Ptgs: prostaglandin-endoperoxide synthase

QoL: quality of life

SD: stable disease

STAT3: signal transducer and activator of transcription 3

TAM: tumor-associated macrophages

TDR: tumor destruction ratio

TGF-β: transforming growth factor-betta

TME: tumor microenvironment

TNBC: triple-negative breast cancer

TNF: tumor necrosis factor

Treg: regulatory T cells

VCAM: vascular cell adhesion molecule

VCAM: vascular cell adhesion molecule

VEGF: vascular endothelial growth factor

2. Introduction

2.1. Modulated electro-hyperthermia as a tumor treatment method

2.1.1. A basic principle of modulated electro-hyperthermia

Modulated electro-hyperthermia (mEHT) is a type of hyperthermia, that represents a non-invasive adjuvant treatment method applied to different types of tumors in clinics [1–3]. It enhances the effectiveness of conventional cancer therapies, such as chemo -, radio-, and immunotherapy [4–8].

mEHT delivers energy using a 13.56 MHz electromagnetic current, generated by a setup consisting of two coupled electrodes. mEHT specifically targets the tumor without affecting healthy neighboring tissues (Figure 1) [9]. The phenomenon can be explained by a metabolic change in cancerous tissue. Instead of 'usual' aerobic glycolysis happening through a citric acid cycle in mitochondria, the tumor is characterized by an increased metabolic rate due to high glucose uptake and energy release through anaerobic glycolysis (Warburg effect) [10]. This leads to lactic acid, metal ions, and salt accumulation in the cytosol and extracellular matrix. These changes significantly enhance the electrical conductivity of the tumor compared to healthy surroundings [11]. High conductive tumor tissue absorbs electric field selectively, which is transformed into heat. The mentioned phenomenon guarantees maintenance of 42 (±0.5) (°C) in the tumor locally and 40 °C in the neighboring tissue [12].

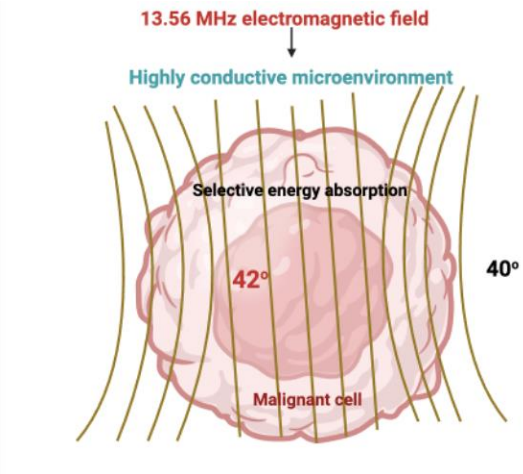

Figure 1. Selective energy absorption by malignant tumor. mEHT uses a 13.56 MHz electromagnetic current to target cancer tissue selectively. The tumor's highly conductive microenvironment, explained by the Warburg effect, absorbs the electromagnetic field, resulting in a temperature gradient - 42 °C in the tumor and 40 °C in the neighboring tissue. *Image created with Biorender.com*

mEHT thermal effect leads to the breaking of double-stranded deoxyribonucleic acid (DNA), which affects the cell cycle and apoptosis [13]. In addition to that, modulated electro-hyperthermia exerts a non-thermal effect through the 1/frequency amplitude modulation of the electromagnetic field. The modulation disturbs cancer cells by inducing the rotation of cell particles. It enhances cell membrane permeability through electroporation and enables more effective drug delivery [4,9].

1.1.1. Clinical and pre-clinical application of modulated electro-hyperthermia

The principle of mEHT treatment in both clinical and pre-clinical settings is similar: mEHT is administered through a device consisting of plan-parallel electrodes (Figure 2 A, B).

mEHT is used in clinics mostly as an adjuvant therapy in combination with conventional anti-cancer therapies. Multiple clinical studies suggest that mEHT treatment is an effective method for tumor growth inhibition in several cancer types, such as

glioblastoma, breast, pancreatic and cervix cancers [14]. The safety profile of the treatment is approved by a clinical study Phase 1 clinical trial, which demonstrated no significant side effects in high-grade glioma patients [15]. Another study evaluated mEHT use in advanced metastatic breast cancer patients, who were irresponsive to any other anti-cancer therapies. 60% of patients demonstrated partial response (PR) or stable disease (SD) to the combination therapy, which may prove that mEHT increased sensitization of the cancer to the conventional treatment [16]. The latest Phase 3 clinical trial gives evidence regarding the efficacy of mEHT in cervical cancer in combination with radiotherapy [17]. mEHT improved both overall response (OR) and quality of life (QoL) of the patients.

The pre-clinical application of mEHT is based on the same principle. However, in addition to the mEHT device, 3 optical sensors let us continuously monitor: body temperature (rectal optical sensor), heating pad, and room temperature (Figure 2 B) [18]. A more detailed description of using the mEHT pre-clinical treatment is given in the methods section.

A

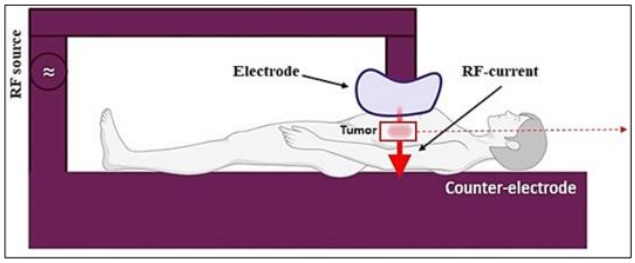

B

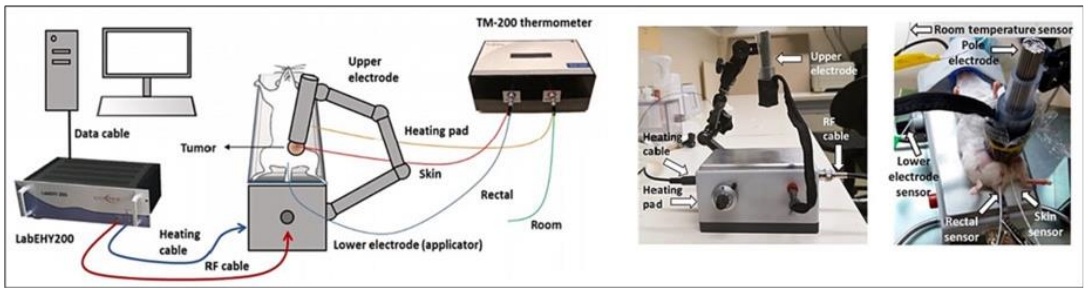

Figure 2. Schematic illustration of clinical (A) and pre-clinical (B) modulated electro-hyperthermia (mEHT) set-up. (A) The patient lying between the plan-parallel electric condenser plates of a clinical mEHT device, which targets the malignant area. Due to metabolic changes in the malignant tissue, its impendence is reduced, causing selective absorption of the electromagnetic field and localized heating. (B) LabEHY200 mEHT treatment setup illustration for *in vivo* mouse experiments by Schvarcz et al.[18] and Danics et al.[19]. The device consists of 3 additional optical sensors for monitoring the heating pad, body, and room temperature.

2.2. Tumor types

2.2.1. Triple-negative breast cancer

Triple-negative breast cancer (TNBC) poses significant challenges in treatment due to its aggressive nature and lack of therapeutic targets [20]. This subtype of breast cancer is characterized by the absence of estrogen receptors (ER), progesterone receptors, and human epidermal growth factor receptor 2 (HER2), making traditional hormonal therapies ineffective against it [21]. As a result, patients with TNBC often have limited treatment options compared to other subtypes of breast cancer. Furthermore, TNBC is associated with

an immune desert phenotype, indicating a lack of immune cell infiltration within the tumor microenvironment [22]. This immune evasion mechanism contributes to the rapid metastasis of TNBC, particularly to organs such as the brain, lungs, and liver [23].

There has been a focus on developing adjuvant therapies that target specific molecular hallmarks associated with TNBC [24]. These targeted therapies aim to disrupt key signalling pathways involved in cancer growth and metastasis [25]. Conventional approaches such as chemotherapy and surgical interventions remain essential components of TNBC treatment, often used in combination with emerging targeted therapies to maximize efficacy [24].

2.2.2. Melanoma

Melanoma incidence has been rising steadily over the past few decades, particularly in fair-skinned populations exposed to excessive ultraviolet radiation [26]. It is an aggressive form of skin cancer. Around 65% of people diagnosed with melanoma face metastasis, which significantly reduces survival rate [27,28]. Contemporary therapeutic approaches involve surgical resection to remove the primary tumor, often followed by chemotherapy [29]. Lately, immunotherapy or tyrosine kinase inhibitors, which disrupt specific signaling pathways involved in melanoma growth and progression, have demonstrated significant benefits in certain patient populations [30,31]. Advanced therapeutical or combination treatments are highly valuable to improve the outcome due to the high metastatic and mortality rates.

2.3. Pro-inflammatory mediators and pathways in cancer development

2.3.1. Cyclooxygenase (COX) isoforms and their biological function

COX enzymes belong to the peroxidase enzyme family and play a critical role in catalyzing the conversion of arachidonic acid (AA) into proteinoids, including prostaglandins (PG), thromboxane, and prostacyclin. These lipid compounds are involved in a wide array of physiological processes, including inflammation, pain, fever, and regulation of blood flow. There are 2 isoforms of COX: COX-1 and COX-2, encoded by prostaglandin-endoperoxide synthase 1 (Ptgs1) and prostaglandin-endoperoxide synthase 2 (Ptgs2) genes, respectively, each with different biological functions [32].

COX-1 is a constitutively expressed enzyme found in most human cells and tissues under normal conditions. Among others, it helps to regulate the production of protective gastric mucus, supports platelet function for blood clotting, and maintains blood flow. In contrast, COX-2 is an inducible enzyme primarily activated by inflammatory stimuli such as cytokines, growth factors, tumor promoters, and microbial endotoxins, and is therefore associated with inflammatory diseases [33]. The most important functional mediator for COX-2 is prostaglandin E2 (PGE2). Upregulated COX-2 and PGE2 are involved in pain sensation, the febrile response, inflammation, tissue injury, and repair [34].

2.3.2. Mechanisms of COX-2 contribution to cancer progression

COX-2 expression is upregulated in various cancer types, including breast, colorectal, lung, and prostate cancer, as well as in premalignant lesions, indicating its significance in early tumorigenesis [35][36].

Evidence suggests that COX-2 promotes tumor growth through prostaglandins, particularly prostaglandin E2. There are diverse functions of PGE2, which favors tumor progression as follows (Figure 3):

- Malignant cells become resistant to apoptosis through the upregulation of the proto-oncogene B-cell lymphoma 2 (Bcl-2) [37,38].
- Angiogenesis through the upregulation of vascular endothelial growth factor (VEGF) [39].
- Metastasis through the upregulation of adhesion molecules [40].
- Invasion through the matrix metalloproteinases (MMP) – MMP-2 and MMP-9, which breaks down the matrix and supports the cell mobility [41].
- Immune evasion through the increase of regulatory T cells (Tregs), the activity of tumor-associated macrophages (TAM), and myeloid-derived suppressor cells (MDSC) [42,43].
- Cancer cell survival and proliferation through the modulation of inflammatory pathways (Interleukin - 1 beta (IL-1β), IL-6, Tumor necrosis factor-α (TNF-α)), mitogen-activated protein kinase (MAPK), mammalian target of rapamycin (mTOR),

nuclear factor kappa B (NF-κB)) and signal transducer and activator of transcription Janus kinase/signal transducer and activator of transcription (JAK/STAT) signaling pathway [44][45][46].

Within the tumor microenvironment (TME), COX-2 promotes tumor growth, proliferation, angiogenesis, metastasis, and immune evasion through the synthesis of prostaglandins, particularly PGE2 [47,48]. PGE2 has been linked to cell proliferation by modulation of the Bcl-2 gene, which is translated to an anti-apoptotic protein. It prevents apoptosis by inhibiting the activity of pro-apoptotic proteins Bax and Bak. PGE_2 modulates the expression of inflammatory cytokines - IL-1β, TNF, IL-6 [49], and inflammatory pathways: mTOR, NF-κB, and MAPK. They support the stability of cancer stem cells and proliferation by the establishment of a pro-tumorigenic immunosuppressive microenvironment [44][45][46].

Moreover, COX-2-derived PGE2 expression plays a role in shaping immune responses within the TME. It helps the recruitment of tumor-associated macrophages (TAMs), myeloid-derived suppressor cells (MDSCs), and regulatory T cells (T-regs) [50]. COX-2/PGE_2 signaling promotes the polarization of TAMs towards a protumor genic M2 phenotype, inhibits the function of cytotoxic T cells and natural killer (NK) cells, and enhances the suppressive activity of T-regs and MDSCs. As a result, COX-2-mediated immune evasion results in immune escape, metastasis, and resistance to immunotherapy in cancer [51,52][42].

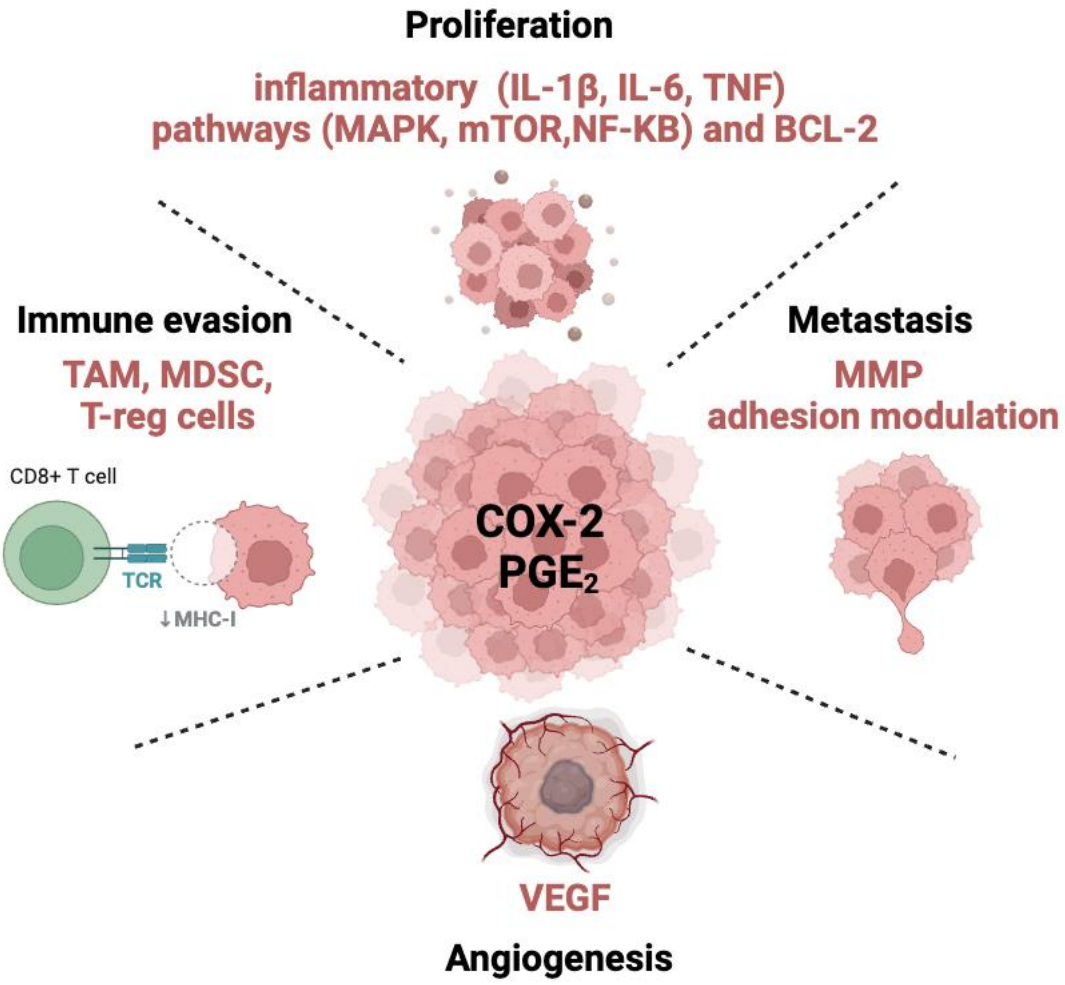

Figure 3. Role of COX-2/PGE_2 signaling within the cancer. COX-2-derived PGE2 modulates tumor cell proliferation via the expression of pro-inflammatory cytokines (IL-1β, TNF, IL-6), activation of inflammatory pathways (MAPK, mTOR, NF-κB), and transcription of the anti-apoptotic gene BCL-2; PGE2 promotes angiogenesis through VEGF; PGE2 supports immune evasion by inhibiting the immune response via activation of TAMs, Tregs, and MDSCs, thereby establishing a pro-tumorigenic and immunosuppressive microenvironment; PGE2 enables metastasis by modulating adhesion molecules and MMPs in the extracellular matrix. *Image created in Biorender.com.*

2.3.3. Anti-cancer therapy induced COX-2 expression and non-steroid anti-inflammatory drugs to overcome the limitation

In the present study, we report that mEHT induced COX-2 synthesis, which we consider as part of the therapy-induced cellular stress reaction. Other anti-cancer therapies, such as chemo- and radiotherapies are also known to cause overexpression of COX-2 and prostaglandins (Figure 4). Bell et al. investigated the COX-2 expression in the 4T1 TNBC after treatment with cisplatin and 5-fluorouracil (5-FU) both *in vitro* as well as *in vivo* [53]. Similarly, radiotherapy can also result in COX-2 overexpression [54,55]. Studies assume COX-2 expression may be considered a self-defensive response of cancer cells due to therapy-induced cellular stress, which limits the anti-cancer therapy's efficacy [56]. Non-steroid anti-inflammatory drugs (NSAIDs) are suggested to overcome the problem as they effectively reduce prostaglandin production by blocking COX-2 enzymatic activity and modulating downstream signaling events [57].

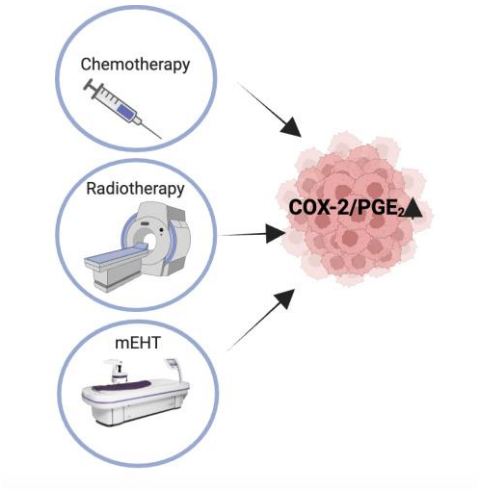

Figure 4. Anti-cancer therapy can induce COX-2/PGE_2 overexpression. Anti-cancer therapies, such as chemo-, radio-, and mEHT therapies induce the increased production of COX-2/PGE_2, which may increase cancer cell resistance and limit treatment efficacy. *Image created in Biorender.com.*

2.3.4. Inflammatory cytokines - IL-6, and IL-1β

Cytokines are a group of soluble secreted protein molecules that are produced in response to changes in the body's normal state, and they carry out their function by interacting

with specific receptors. Cytokines can be divided into two large groups: pro-inflammatory cytokines (IL-1β, IL-6, TNF-α, IL-17) and anti-inflammatory cytokines (IL-10, interferon-alpha (IFN-α), transforming growth factor-beta (TGF-β), IL-4, IL-13) [58]. There is a strong positive feedback loop between COX-2 expression and pro-inflammatory cytokines, IL-6 and IL-1β, as they stimulate each other's synthesis [44][59][35].

IL-6 is considered a malignancy and a prognostic marker for overall survival in several cancers [60]. It binds to IL-6Rα coupled with co-receptor - glycoprotein 130 (gp130). Due to activating signaling pathways, such as the JAK/STAT signaling pathway, IL-6 promotes proliferation and inhibits apoptosis. The IL-6/JAK/STAT pathway is understood as tumor-promoting and represents a target of the latest anti-cancer treatment development [61].

IL-1β exerts its biological function via interacting with IL-1 receptors (IL-1Rs). IL-1β is upregulated in various cancer types, such as breast, melanoma, head, colon, and lung cancers and it is associated with worse prognosis [62]. It acts as a growth factor and enhances the overexpression of other proinflammatory cytokines (TNF, IL-6), pathways (MAPK, NF-κB), adhesion molecules (Intercellular Adhesion Molecule (ICAM), Vascular Cell Adhesion Molecule (VCAM)), and growth factors such as VEGF, therefore IL-1β synergistically works with other factors and promotes inflammation, angiogenesis, and metastasis [63].

Overall, IL-6 and IL-1β are key regulators of the TME, exerting pleiotropic effects on cancer progression and immune responses [64]. Their expression is associated with increased inflammation, cell proliferation, angiogenesis, and resistance to apoptosis [65](66). Targeting IL-6 and IL-1β and their signaling pathways represents a promising therapeutic approach to disrupt the pro-tumorigenic TME, enhance anti-tumor immune responses, and improve patient outcomes in cancer treatment [64] [56] [66].

2.4. Cyclooxygenase inhibitors and cancer therapy

2.4.1. COX-1 and COX-2 inhibitors - mechanism of action

COX inhibitors are divided into 2 main groups: non-selective non-steroid anti-inflammatory drugs (NSAIDs) (aspirin) and selective COX-2 non-steroid anti-inflammatory drugs (SelCOXIBs) (Figure 5). They contribute anti-inflammatory, antipyretic, and analgesic

effects. NSAIDs bind to the COX active site, that is created by a long hydrophobic channel and prevents catalyzing arachidonic acids to prostaglandins [67].

Acetylsalicylic acid (aspirin, ASA) is synthesized from the natural compound - salicylic acid. It can irreversibly inactivate COX-1 and COX-2 due to acetylation but inhibits COX-1 more than COX-2. COX-1 is involved in platelet aggregation; therefore, aspirin is used in cardiovascular protection. Inhibition of COX-1 in the long term may cause a significant gastrointestinal side effects, such as gastritis, stomach ulceration, and bleeding[67].

selCOXIBs are designed for COX-2 inhibition, while sparing COX-1. They have demonstrated a better anti-inflammatory effect, but also a risk of increased cardiovascular adverse events [68].

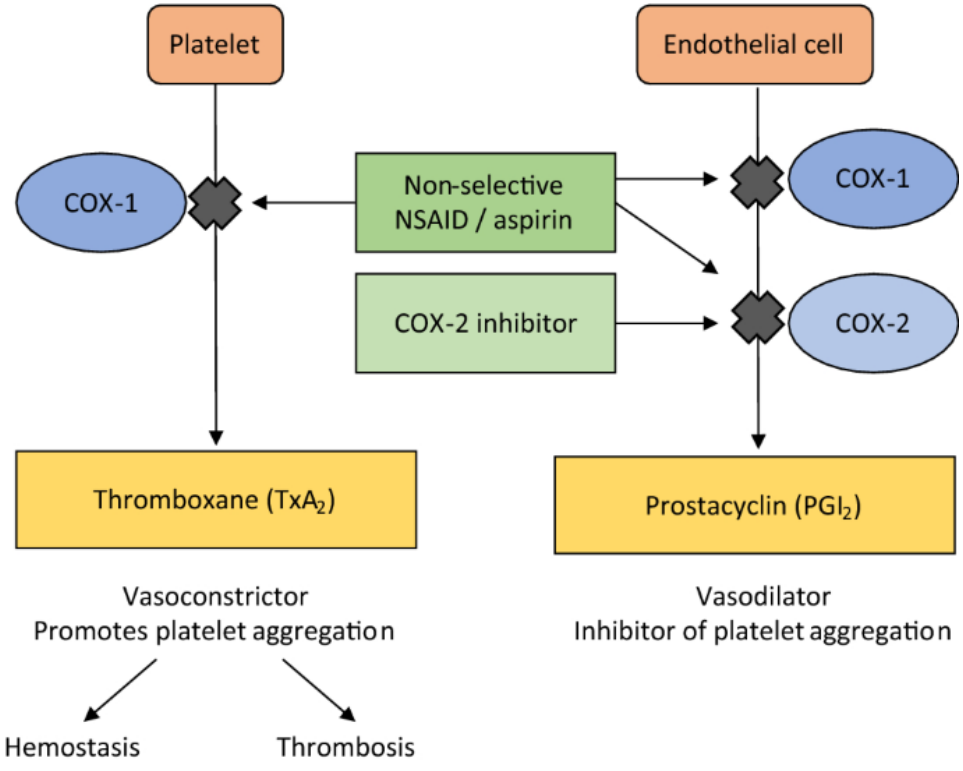

Figure 5. non-selective COX and selective COX-2 inhibitors effect on endothelial cells and platelet aggregation [69].

2.4.2. Non-selective COX and selective COX-2 inhibitors in cancer therapy

Numerous epidemiological and experimental studies show that NSAIDs reduce the risk, incidence, and mortality in some cancers [70], including melanoma [71] and breast cancer [72]. Both non-selective and selCOXIBs have been associated with lower cancer incidence, however, selCOXIBs have demonstrated greater significance [73]. NSAIDs inhibit the production of prostaglandins and pro-inflammatory cytokines [74], tumor growth factors [43,45,75] and inflammatory pathways such as NF-κB [76], MAPK [77], mTOR [78], PDK-1/Akt [79], Wnt/β-catenin [80]. These pathways support cell proliferation and angiogenesis but suppress apoptosis. Therefore, COX inhibitors influence tumor progression by decreasing migration [81], metastasis [82,83], angiogenesis [84], increasing apoptosis and sensitivity to other conventional anti-cancer therapies such as chemotherapy, immunotherapy, or radiotherapy [85,86] (Figure 6).

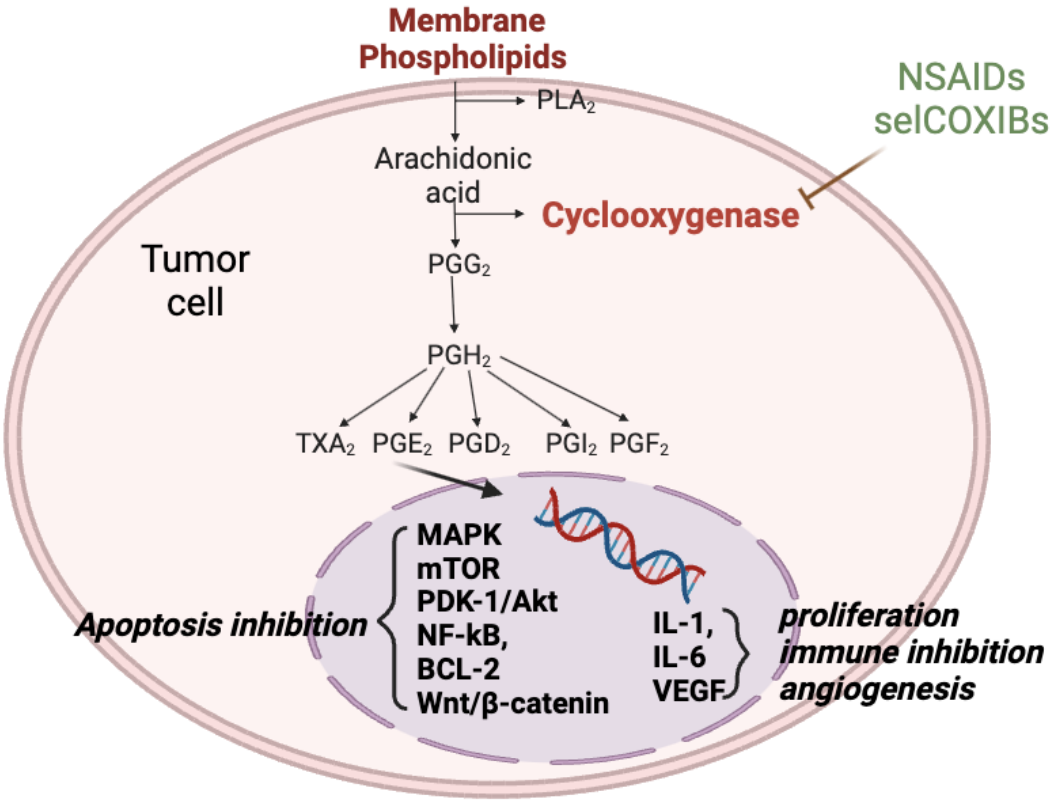

Figure 6. The underlying mechanism of COX inhibition - NSAIDs and selCOXIBs regulate signaling pathways in cancer cells. NSAIDs inhibit prostaglandin synthesis through the COX inhibition. COX inhibition modulates pro-inflammatory cytokines (IL-1β, IL-6), and inflammatory pathways such as NF-κB, MAPK, mTOR, PDK-1/Akt, and Wnt/β-catenin by the inhibition of activation of transcription factors. These pathways support cell proliferation, immune evasion, and angiogenesis but suppress apoptosis. *Image created in Biorender.com*

2.4.3. Combination of COX-2 inhibitors with other anti-cancer therapies

Various studies have demonstrated that COX-2 inhibition, when combined with cancer treatments, significantly enhances outcomes against cancer (Table 1). The table offers a summary of combination treatments of COX inhibitors and possible synergistic mechanisms of action.

Table 1. Studies on the combined use of COX-2 inhibitors in the treatment of human cancers.

Summary of combined treatments with COX inhibitors and possible synergistic mechanisms of actions *based on the review paper Rodrigues P, Bangali H et al 2024* [87]

Combination	**Cancer type**	**Effect(s)**	**Mechanism/Signaling pathway**	**References**
Celecoxib and cyclophosphamide	Breast cancer	Anti-angiogenic	Decrease VEGF	[88]
Celecoxib and 5-FU	Squamous cell carcinoma	Inhibit proliferation	Inhibit AKT pathway	[89]
Celecoxib and epirubicin	Novikoff hepatoma	Reduce proliferating	Suppress CD44, CD133 and	[90]

			MDR-1 expression	
Celecoxib and doxorubicin	Human skin cancer	Enhance apoptosis	Inhibit AKT pathway	[91]
Celecoxib and rapamycin	Gastric cancer	Increase sensitivity	Inhibit PI3K/AKT pathway	[92]
Celecoxib and doxorubicin	Drug-resistant breast cancer	Induce apoptosis	Inhibit P-gp expression	[93]
Celecoxib and curcumin	HCC	Inhibit angiogenesis	Inhibit Akt, NF-κB , and PGE2	[94]
Tolfenamic acid and cisplatin	Breast cancer	Induce apoptosis	Increasing P-53	[95]
Celecoxib and erlotinib	NSLC	Enhance apoptosis and radio-sensitivity	Inhibit EGFR and PIK/AKT pathway	[96]
Celecoxib and gefitinib	NSLC	Induce apoptosis	Inhibit EGFR pathway	[97]
Celecoxib and gefitinib	Prostate cancer	Enhance apoptosis/reduce tumor proliferation	Increased caspase 3 cleavage/ decreases in BCL-2 and ABCB1 expression	[98]

Celecoxib and imatinib	Colon cancer	Inhibit proliferation	Increase Caspase-3 activity	[99]
Celecoxib and sunitinib	Renal cancer	Immunomodulation/ Alleviate tumor progress	Inhibit GM-CSF and STAT3 expression/Alleviating MDSCs	[100]
Celecoxib and sorafenib	Ovarian cancer	Induce apoptosis/	Reduce chaperone proteins	[101]
Celecoxib and sildenafil	Ovarian cancer	Induce apoptosis/Increased platinum sensitivity	Reduce chaperone proteins	[101]

2.5. Endothelial marker CD105 and its role in angiogenesis

CD105, also known as endoglin, is a transmembrane glycoprotein predominantly expressed on the surface of endothelial cells. It serves as a crucial component in the regulation of angiogenesis and cellular responses to TGF-β signaling [102]. It has a role in vascular development and repair and has significant implications in pathological conditions such as cancer and fibrotic diseases [103]. In oncology, targeting CD105 with monoclonal antibodies or small molecules could effectively hinder tumor angiogenesis, thereby starving the tumor of its blood supply and inhibiting its growth. Clinical trials investigating anti-CD105 therapies, such as TRC105, have demonstrated potential in treating various cancers by disrupting the angiogenic processes, although the exact mechanism is not fully understood [104].

3. Objectives

Our aims were:

1. To investigate the molecular effects of mEHT in the treatment of 4TI TNBC.
2. Understanding the role of mEHT-induced COX-2, IL-6, and IL-1β expression in 4T1 TNBC.
3. To enhance the anti-tumor effect of mEHT - establish a protocol for 4T1 TNBC and B16F10 melanoma mouse models using combinational treatment of mEHT and COX inhibitors.
4. To gain new, translationally relevant insights that can be used in clinical therapy.

4. Materials and methods

4.1. Cell culture

B16F10 cells (B16-F10 (RRID: CVCL_0159)) melanoma cell line was purchased from ATCC (ATCC®CRL 6475TM; Manassas, VA, USA), 4T1 (4T1 (RRID: CVCL_0125)) TNBC mouse cell line was provided by Judy Lieberman (Lieberman Laboratory, Harvard University, Boston, MA, USA). Cells were cultured according to protocols described in the previous studies [18,105]. In brief, 4T1 cells were grown as adherent cultures in a medium (DMEM, 4.5 g/L glucose without L-glutamine and Phenol Red, Capricorn Scientific, Ebsdorfergrund, Germany) supplemented with 10% Fetal Bovine Serum (FBS (South America Origin), EU approved, Euroclone S.p.A. Pero, Italy), L-glutamine 200 mM (Capricorn Scientific, Ebsdorfergrund, Germany), and penicillin 100x (Capricorn Scientific, Ebsdorfergrund, Germany). The B16F10 cells were cultured in MEM (Minimum Essential Medium) supplemented with 1% (v/v) MEM-vitamin solution, 5% (v/v) heat-inactivated HyClone fetal bovine serum, 1 mM sodium pyruvate, 2 mM L-glutamine, and 1% (v/v) nonessential amino acids (NEAAs) purchased from Thermo Fisher Scientific (Waltham, MA, USA). Regular mycoplasma screening was conducted on all cell lines, and all experiments were carried out using mycoplasma-free cells.The cell lines underwent authentication in the past three years through multiple evaluations, comparing newly acquired data with well-established databases and reference panels. The process ensures the ongoing verification and validation of cell line identities.

4.2. Animals housing

Female BALB/c and C57BL6/ mice, aged 5 weeks, were ordered from the National Institute of Oncology (Budapest, Hungary) and housed under minimal disease conditions at the Animal Facility of the Basic Medical Science Center of Semmelweis University with free access to standard mouse chow and tap water ad libitum and under a 12 h dark/light cycle. Interventions and animal housing were carried out in accordance with Hungarian Law Nos. XXVIII (1998 and 2002) and LXVII (2002), both of which deal with animal protection and welfare, as well as European Union guidelines. The National Scientific Ethical Committee

on Animal Experimentation approved all animal treatments under the code PE/EA/50-2/2019 on November 1, 2019.

4.3. *In vivo* treatment of 4T1 TNBC

1×10^6 4T1 TNBC cells /50µl PBS (Phosphate Buffered Saline with no Magnesium and Calcium, , Lonza A. G., Basel, Switzerland) were aspirated into Hamilton syringe (Hamilton Company, Reno, NV, USA), Mice were inoculated in the 4th mammary fat pad at the age of six- to eight-weeks In brief, isoflurane (Baxter International Inc., Deerfield, IL, USA) was used to anesthetize animals: for induction - 4-5% and for maintenance - 1.5-2%. 4T1 tumor cells were subcutaneously injected in each mouse's inguinal mammary fat pad using compressed air (0.4-0.6 L/min). On the eighth day after tumor injection, tumor volume was measured using ultrasound, as described previously [19]. Mice were randomized according to tumor volume into six different groups. On the same day, animals were given a daily dose of 100 mg/kg acetylsalicylic acid (Aspirin, ASA, Sigma-Aldrich Co., St. Louis, MO, US.) or 6 mg/kg selective COX-2 inhibitor (SC236, Axon Medchem BV, Groningen, The Netherlands) via intraperitoneal injections [82]. Drugs were dissolved in 10% DMSO, 40% PEG300, 5% Tween-80, and 45% saline. Treatment with COX inhibitors, administered every day during the entire experiment, was combined with mEHT (Figure 7 A). Mice were treated four times in every 48 hours with a newly constructed labEHY-200 mEHT device (Oncotherm Ltd., Páty, Hungary) or Sham as detailed in our prior publications [18,19]. Tumor volume was monitored by ultrasound and digital caliper every day until the termination of the experiment.

In two separate experiments, we investigated the long-term effects of mEHT treatment. In the time-kinetic experiment (Figure 7 B), mice were treated with mEHT and tumors were harvested after 3 mEHT treatments at different time-points. In the long-term follow-up experiment (Figure 7 C), tumors were harvested 96 hours after 2 mEHT treatments. The mice were euthanized by cervical dislocation on the day after the last treatment. Tumors were excised and cleaned for further processing. Half of the tumors were fixed in a 4% formaldehyde solution (Molar Chemicals Ltd., Halásztelek, Hungary), the other half was cut and stored at -80 °C for molecular analysis.

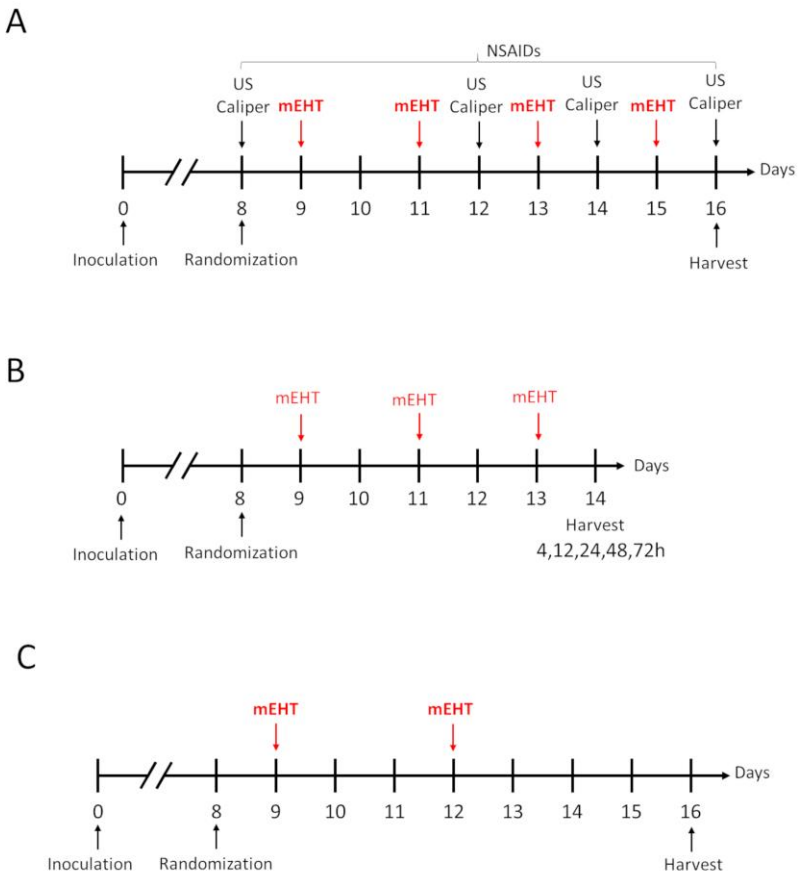

Figure 7. Experimental protocols of the 4T1 model. 4T1 triple-negative breast cancer (TNBC) cells were inoculated at the day zero. Mice were randomized at day eight. Modulated electro-hyperthermia (mEHT) treatments and NSAID administeration were performed every day from randomization until the end of the experiment. Ultrasound and caliper tumor volume measurements were performed on every intermittent day. Tumors were harvested at the end of the study. (A) Combination therapy: 4x mEHT treatment in combination with Aspirin or SC236. (B) Time kinetic experiment: 3x with mEHT treatment + tumor harvest at different time points. (C) Long-term follow-up: 2xmEHT treatment + tumor harvest at 96h after the last treatment.

4.4. In vivo treatment of B16F10 melanoma

1×10^5 B16F10 melanoma cells were injected into the tail vein of female C57BL/6 mice, which induced tumor nodules in the lungs. The mice were randomized based on body weight.

One day after inoculation, mice were treated with mEHT alone or mEHT combined with aspirin at 11.1 mmol/L concentration in their drinking water [106]. Because aspirin insoluble in water, aspirin was dissolved in 0,2 % DMSO and then mixed with the drinking water using a magnetic mixer. pH was adjusted to 7.4 - physiological pH using a combination of NaOH and/or HCl and a pH meter. Animals have been six times treated with the LabEHY-200 device set up to maintain 41–42 °C inside the mice's lungs [105]. According to the protocol, 30 min mEHT treatments were repeated six times in total on every third day (Figure 8). Animals were terminated on day 20, 48 hours after the last mEHT treatment. The burden of lung melanoma was assessed by counting the number of tumor nodules on the lung surface [105].

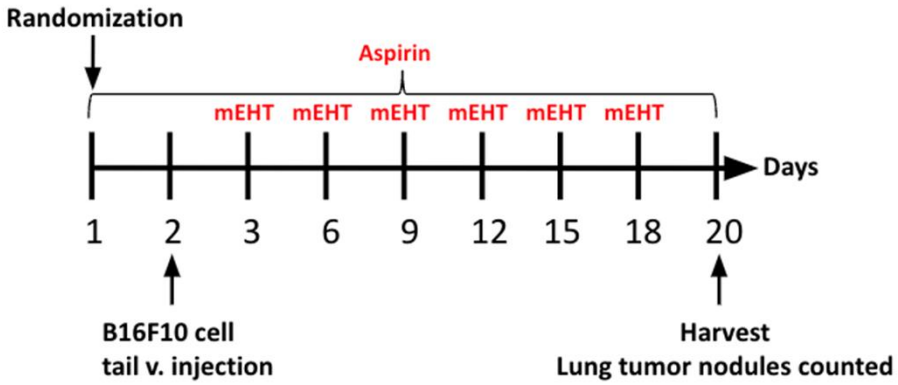

Figure 8. Experimental protocol of the B16F10 melanoma experiment. Randomization was performed at day 1, B16F10 melanoma cell were inoculated through the tail vein at day 1, modulated electro-hyperthermia (mEHT) treatments were performed at day 2, 5, 8, 11, 14 and 17. Aspirin mEHT combined with aspirin at 11.1 mmol/L concentration in their drinking water was administered every day from day zero until the end of the experiment. Tumors were harvested at day 20.

4.5. Real-time PCR after RNA isolation

RNA was isolated using TRI reagent (Molecular Research Center Inc., Cincinnati, OH, USA) according to protocol provided by the manufacturer. A high-capacity cDNA reverse transcription kit was used to reverse transcribe the isolated RNA (Applied Biosystems, Carlsbad, CA, USA). The amplified cDNA was used as template for the RT-PCR. SYBR Green-based qRT-PCR using Sso Advanced ™ Universal SYBR® Green Supermix and the CFX96 Touch Real-Time PCR Detection System was used to detect messenger RNA in the samples (Bio-Rad, Hercules, CA, USA). The 18S and GAPDH genes were used as normalising genes (Table 2).

Table 2. Primer Pair designed for RT-PCR

Gene Symbol	**Gene Name**	**Primer Pair**
18S	18S (Mus musculus)	Fwd: CTCAACACGGGAAACCTCAC Rev: CGCTCCACCAACTAAGAACG
GAPDH	glyceraldehyde-3-phosphate dehydrogenase (Mus Musculus)	Fwd: CTCCCACTCTTCCACCTTCG Rev: GCCTCTCTTGCTCAGTGTCC
IL-1β	Interleukin 1 beta (Mus Musculus)	Fwd: ACCTGTTCTTTGAGGCCGACA Rev: CCACAGCCACAATGAGTGAC
IL-6	Interleukin 6 (Mus Musculus)	Fwd: GATGCTACCAAACTGGATATAA TC Rev: GGTCCTTAGCCACTCCTTCTGTG

COX-2	Ptgs2 (Mus Musculus)	Fwd: TCACGTGGAGTCCGCTTTAC Rev: AGGATGCAGTGCTGAGTTCC

4.6. Immunohistochemistry and histopathology

The tumor tissues were preserved in 4% formalin and then encased in paraffin (FFPE). Using a polymer-peroxidase system (Histols, Histopathology Ltd., Pécs, Hungary), we cut serial sections of 2.5 μm, dewaxed, and rehydrated them for hematoxylin-eosin (HE) staining or immunohistochemistry (IHC) (Table 3). The viable tumor area per cross-sectional tumor area was determined using the QuantCenter image analysis software (3DHISTECH), and the tumor destruction ratio (TDR%) was determined by dividing the necrotic area by the whole tumor area [19].

Table 3. Antibodies and conditions used for immunohistochemistry

Antigen	**Type**	**Reference no.**	**Dilution**	**Vendor**
cCasp3	Rabbit, pAb	#9664	1:1600	Cell Signaling

4.7. Nanostring

Extracted RNA was used for RNA detection with Nanostring technology (Nanostring, Redwood, CA, USA). Nanostring uses unique optical barcoded RNA that hybridize to the target RNA in the sample to enable digital counting of individual RNA molecules without possible artefacts introduced by enzymatic steps. The gene expression panel was custom made based on our previous publication in which mEHT-regulated genes were detected by next generation sequencing (NGS) and verified by Nanostring. The custom panel composed of 134 genes [18].

In brief, 100 ng RNA was used for hybridization. After hybridization, samples were transferred to the nCounter Prep Station for data collection on the nCounter Digital Analyzer. The 4.0 nSolver Analysis Software (Nanostring, Redwood,CA, USA) was used for data analysis. Genes with $\log_2$ fold change values greater than 1.5 or less than -1.5 were considered the most regulated for further analysis. Values obtained from three replicates of two groups, mEHT or mEHT+SC236, were used to generate the volcano plot. DEGs was conducted utilizing the Gene Ontology (GO) which was accessed through the DAVID [107]. GO analysis was used to identify genes that can be classified into different groups. In our study, we used the database for DAVID (https://david.ncifcrf.gov/) to perform functional annotation clustering the most regulated genes. The p-value represents the probability of chance association between genes and a specific functional category. The p-value was adjusted with the Benjamini-Hochberg procedure to control for false discovery rate (FDR) by correcting for multiple comparisons.

4.8. Statistical data analysis

The statistical analysis was conducted using GraphPad Prism software (v.6.01; GraphPad Software, Inc., La Jolla, CA, USA). Unpaired Mann-Whitney non-parametric tests were used to compare the Sham and the mEHT-treated groups. Long-term examinations were statistically evaluated with one-way ANOVA. The data are presented as mean ± SEM. Differences were considered statistically significant if $p < 0.05$.

5. Results

5.1. mEHT induced IL-1β, IL-6, and COX-2 mRNA expression

mEHT induced the expression of pro-inflammatory cytokines (IL-6, IL-1β) in 4T1 TNBC *in vivo*. In the time-kinetic experiment, mice were terminated after the last mEHT treatment at 4h, 12h, 24h, 48h and 72h (Figure 9 A). IL-6 (Figure 9 B) peaked at 12 hours (p=0.007), while IL-1β (Figure 9 C) peaked at 24 hours after the last mEHT treatment (p=0.009). IL-6 was 3.8- and IL-1β 3 times higher in the mEHT-treated mice vs Sham. COX-2 mRNA was significantly elevated at 72h after the last mEHT session (p=0.01) (Figure 9 D) and was increased even at 96 hours (Figure 9 F) after 2X mEHT treatment.

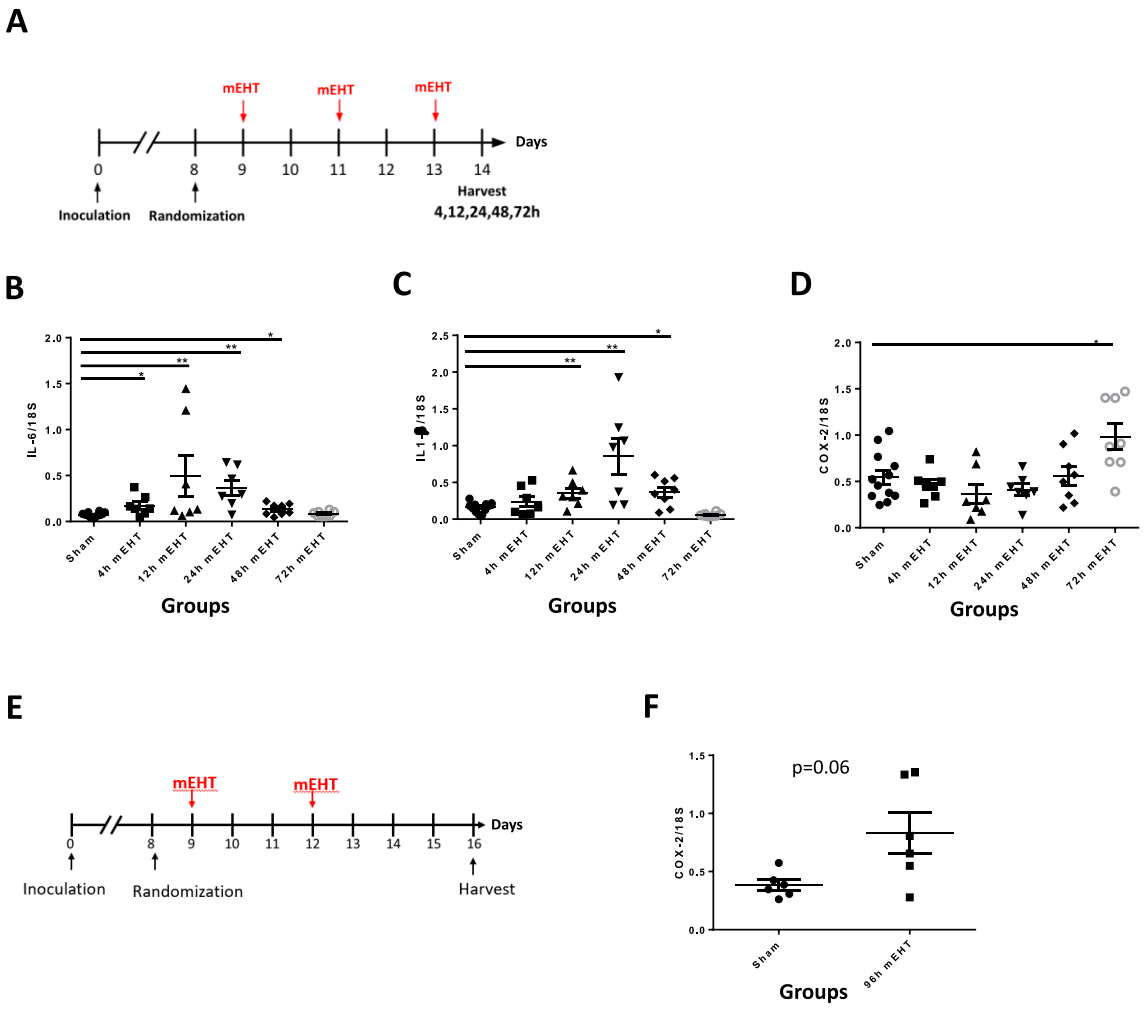

Figure 9. Time kinetics of proinflammatory cytokines' mRNA after modulated electro-hyperthermia (mEHT) treatment. (A) Experimental protocol of the time kinetic experiment. (B, C, D) – mice were treated 3 times with mEHT and terminated at 4, 12, 24, 48 and 72h after last treatment. Inflammatory cytokines expression was measured using qRT-PCR: (B) IL-6. (C) IL-1β. (D) COX-2. (E) Protocol of the long-term follow-up experiment (G) – mice treated twice with mEHT and terminated at 96h, and COX-2 expression was measured. (F) COX-2 mRNA 96h after two mEHT treatments (p=0.06). Expression normalized to 18S reference gene. Values are expressed as mean±SEM, Unpaired Mann–Whitney test *: p< 0.05, **: p< 0.01. Number of animals/groups: (B – D) Sham-each timepoint:12, mEHT- 4h:6; 12,24h:7; 48,72h:8; (F) 96h: Sham:6; mEHT: 6.

5.2. mEHT disrupts blood vessels with following recovery seen in the endothelial marker CD105 expression in 4T1 TNBC

mEHT treatment significantly downregulated CD105 expression at 12h (p=0.0002) compared to the Sham treated group, however, its expression returned to the Sham level afterwards (Figure 10).

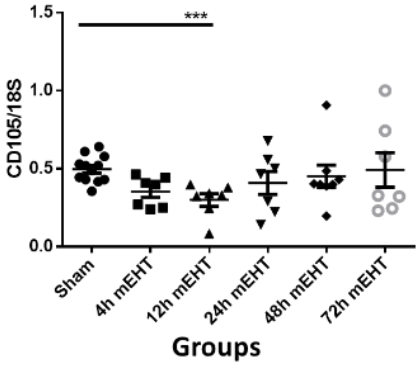

Figure 10. Time kinetics of CD105 mRNA after modulated electro-hyperthermia (mEHT) treatment). Expression is normalized to 18S reference gene. Values are expressed as mean±SEM, Unpaired Mann–Whitney test ***: p< 0.001 Number of animals/groups: Sham-each timepoint:12, mEHT- 4h:6; 12,24h:7; 48,72h:8;

5.3. mEHT induced expression of IL-1β, IL-6 and COX-2 was inhibited by NSAIDs

In a separate experiment, mEHT and NSAID combination therapy was investigated (Figure 11 A). The mRNA level of IL-1β and COX-2 were upregulated (3.8x and 2.5x, respectively) 24h after the 4 mEHT treatments. IL-1β induction was almost completely reversed to the Sham level using SC236, but not aspirin (Figure 11 B), whereas COX-2 induction was reversed by both SC236 and Aspirin (Figure 11 C).

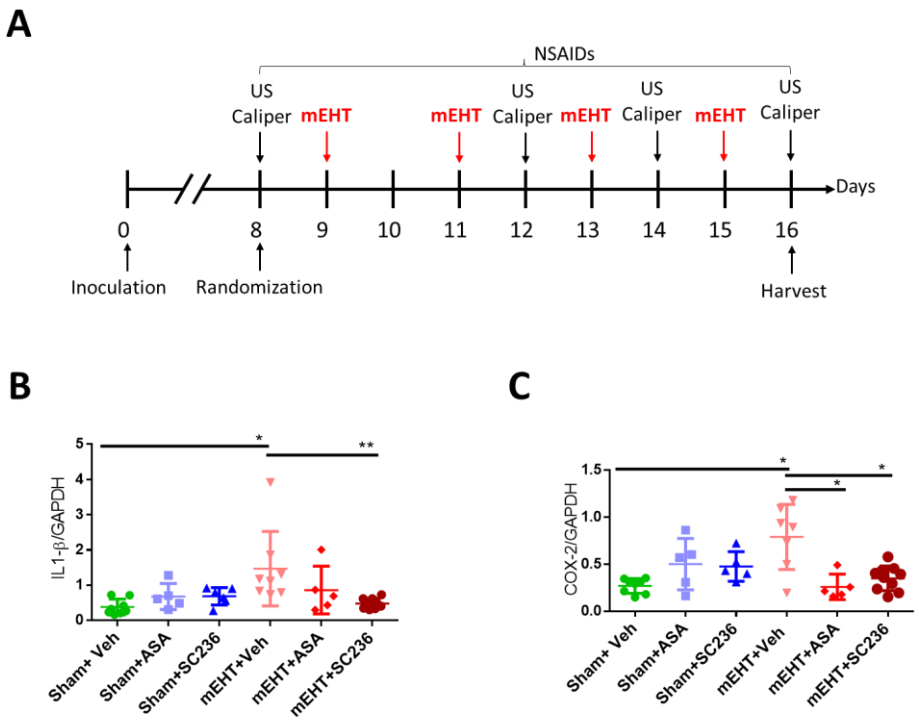

Figure 11. Pro-inflammatory cytokine mRNA after 4-time treatment with modulated electro-hyperthermia (mEHT) and NSAID. (A) Experimental protocol. (B) Expression of IL-1β. (C) Expression of COX-2. Expressions are normalized to GAPDH. One-way ANOVA, Values are expressed as mean±SEM, *: $p< 0.05$, **: $p< 0.01$. Number of animals/groups: (B – C) Sham+Veh:6; Sham+ASA:5; Sham+SC236:5; mEHT+Veh:8; mEHT+ASA:5; mEHT+SC236:10.

5.4. mEHT inhibited tumor growth was accelerated by NSAID co-treatment

During the experiment of mEHT and NSAID combination therapy experiment (Figure 12 A) tumor volumes were assessed by ultrasound. Tumor volumes progressed in Sham+vehicle treated mice from 264 ± 67 mm^3 (after 2 treatments) to 320 ± 59 mm^3 (after 3 treatments) and to 413 ± 77 mm^3 (after 4 mEHT treatments) (Figure 12 B, C, D, G). Monotherapy mEHT +vehicle was able to significantly reduce tumor size after 3 mEHT treatments (p=0.006) (Figure 12 C). Average volume in the mEHT-treated group was 258 ± 54 mm^3 compared to 320 ± 59 mm^3 in the Sham-treated group. However, the combination therapy (mEHT+ASA and mEHT+SC236) was able to significantly reduce tumor volume already after 2 mEHT treatments to 156 ± 51 mm^3 (p=0.02) and 145 ± 49 mm^3, respectively, (p=0.02) compared to the Sham-treated group with an average volume of 264 ± 67 mm^3 (Figure 12 B). After 4 treatments, only the COX-2 specific combination (mEHT+SC236) with 166 ± 54 mm^3 average volume proved to be significantly more effective than mEHT monotherapy (average volume 285 ± 77 mm^3). The COX-2 specific combination (mEHT+SC236) was the most effective inhibitor of tumor growth (Figure 12 G). This observation was supported by significant reduction of the tumor weight at the end of the study (Figure 12 E, F). Average tumor weight in the mEHT treated group was 284 ± 88 mg, while in the mEHT+SC236 it was only 175 ± 51 mg (p=0.04).

Most mice lost not more than 5-10% of their bodyweight by the 3rd treatment, and all recovered by the end of the study. The body weight loss was not significantly different between the groups. Sham treated mice (20.1 ± 1 g) lost an average of 0.5 grams (19.6 ± 0.6 g) by the 3rd treatment. The mEHT treated group (19.4 ± 1.5 grams) lost an average of 1.7 g (17.7 ± 1.6 g). Animals that received the combination treatment of mEHT and ASA (20.7 ± 0.7 g) lost only 1.2 g (19.5 ± 0.6 g), while those treated with mEHT+SC236 (20.7 ± 1 g) did not lose weight (Figure 12 H). Bodyweight by the end of the study did not differ significantly from the initial bodyweight in any of the groups.

A

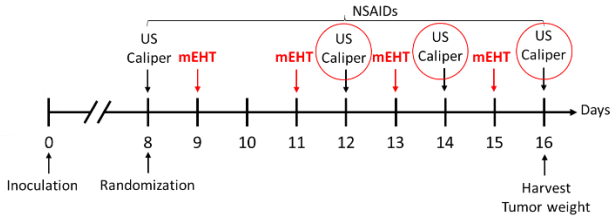
NSAIDs
US Caliper
mEHT
US Caliper
US Caliper
US Caliper
Days
0
8
9
10
11
12
13
14
15
16
Inoculation
Randomization
Harvest Tumor weight

B

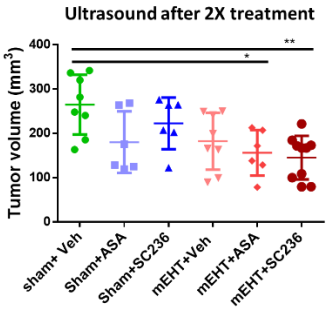
Ultrasound after 2X treatment
Tumor volume (mm3)
sham+ Veh
Sham+ASA
Sham+SC236
mEHT+Veh
mEHT+ASA
mEHT+SC236

C

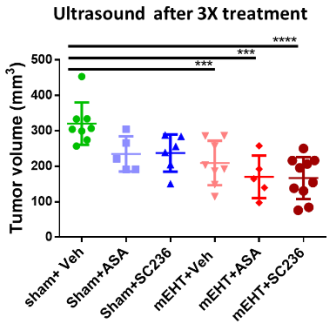
Ultrasound after 3X treatment
Tumor volume (mm3)
sham+ Veh
Sham+ASA
Sham+SC236
mEHT+Veh
mEHT+ASA
mEHT+SC236

D

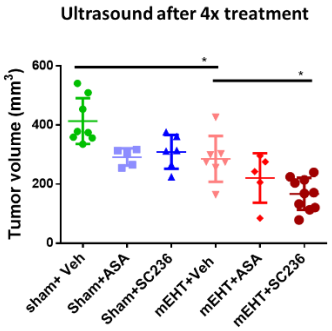
Ultrasound after 4x treatment
Tumor volume (mm3)
sham+ Veh
Sham+ASA
Sham+SC236
mEHT+Veh
mEHT+ASA
mEHT+SC236

E

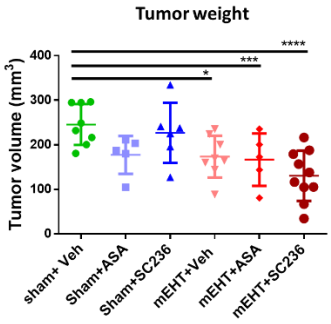
Tumor weight
Tumor volume (mm3)
sham+ Veh
Sham+ASA
Sham+SC236
mEHT+Veh
mEHT+ASA
mEHT+SC236

F

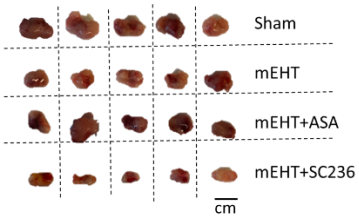
Sham
mEHT
mEHT+ASA
mEHT+SC236
cm

G

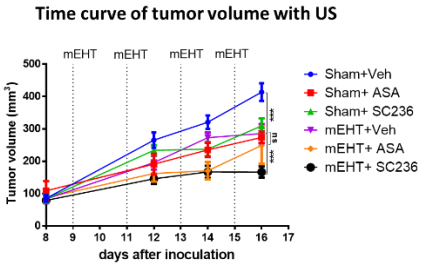
Time curve of tumor volume with US
mEHT
Tumor volume (mm3)
days after inoculation
Sham+Veh
Sham+ ASA
Sham+ SC236
mEHT+Veh
mEHT+ ASA
mEHT+ SC236

H

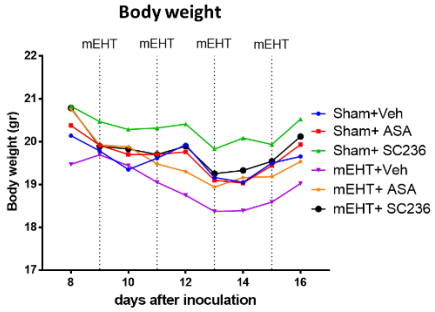
Body weight
mEHT
Body weight (gr)
days after inoculation
Sham+Veh
Sham+ ASA
Sham+ SC236
mEHT+Veh
mEHT+ ASA
mEHT+ SC236

Figure 12. Tumor growth, tumor weight and bodyweight. (A) Experimental protocol. Red circles: US data taken after the 2nd, 3rd and 4th modulated electro-hyperthermia (mEHT) are given on fig. 5/B, C, D, G. Tumor volume after (B) 2, (C) 3 and (D) 4 mEHT treatments. (E) Tumor weight (milligrams) at the end of the experiment. (F) Representative images of all excised tumors (Scale bar, 1 cm). Time curves of tumor growth measured by (G) ultrasound. (H) Body weight (grams). Values are expressed as mean±SEM. One-way ANOVA, Mean ± SEM, *: $p< 0.05$, **: $p< 0.01$, ***: $p< 0.001$, ****: $p< 0.0001$.

5.5. mEHT-induced tumor tissue destruction proved to be cC3-dependent apoptosis that was enhanced by NSAIDs

H&E staining was performed on tumor samples taken after the termination of the mEHT and NSAID combination therapy experiment (Figure 13 A). Pale areas (dead cells) on the H&E-stained slides (Figure 13 B) are corresponding to cleaved caspase-3 positive areas on the immunohistochemistry slides (Figure 13 C), designated as destructed areas appeared on Sham-treated tumors (TDR=52 ± 11 %). mEHT monotherapy (TDR=56 ± 5 %, p=0.9) or in combination with aspirin (TDR=66 ± 10 %, p=0.4) increased the TDR% to some extent, however, these did not reach statistical significance. Significant increase of the TDR was only achieved in the group treated with mEHT + SC236 (TDR=75 ± 14 %). The TDR in the mEHT + SC236 group was significantly different from the mEHT monotherapy group

(Figure 13 D).

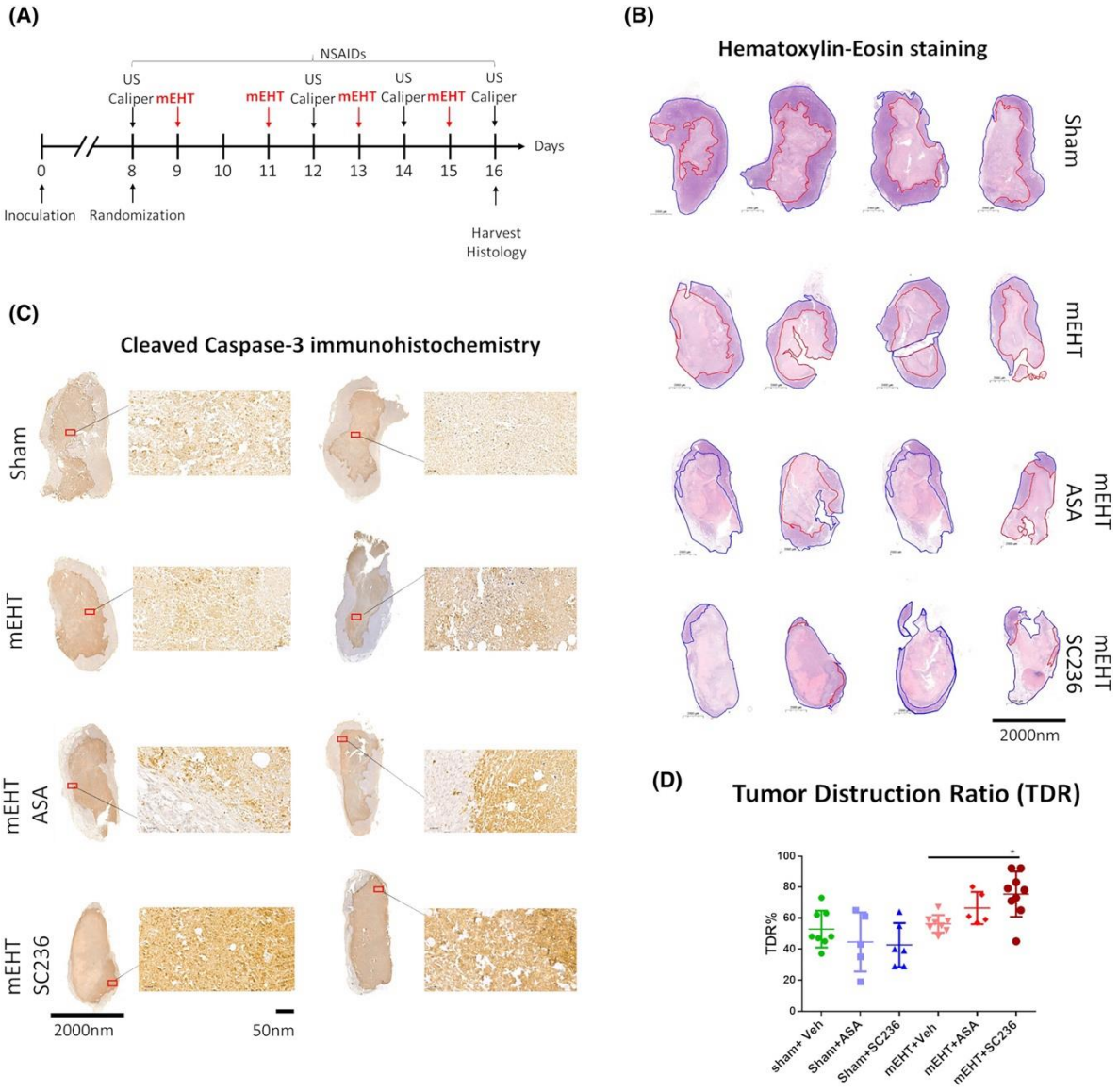

Figure 13. Tumor destruction ratio (TDR%) and cleaved caspase 3 (cC3) staining in harvested tumors. (A) Experimental protocol. (B) Representative pictures of H&E-stained tumors - tumor destruction ratio (TDR%) (red annotation) of whole tumors (blue annotation). (C) Representative pictures of cC3 stained tumors. (D) Quantification of tumor destruction ratio (TDR%). (Magnification: 40 x) One-way ANOVA, Values are expressed as mean±SEM, *: $p < 0.05$.

5.6. Multiplex (Nanostring) analysis demonstrated that COX-2 inhibition negatively correlated with tumor promoting factors associated with tumor cell membrane and extracellular matrix

Three samples from the mEHT and mEHT+NSAIDs experiment (Figure 14 A) passed the Nanostring quality control (QC) and the Nanostring run was successful. 74 genes were identified as differentially expressed (DE) that are displayed on the heat map (Figure 14 B). The most regulated genes are presented individually (red dots) on the volcano plot (Figure 14 C). Genes were identified (Table 4) and clustered in two groups using DAVID. 7 genes were identified as membrane proteins and 6 genes as secreted proteins. The P value and the p-value calculated with the Benjamini-Hochberg procedure is also given on (Figure 14 D).

A

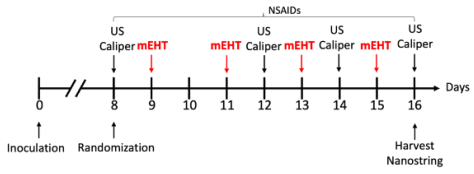

B

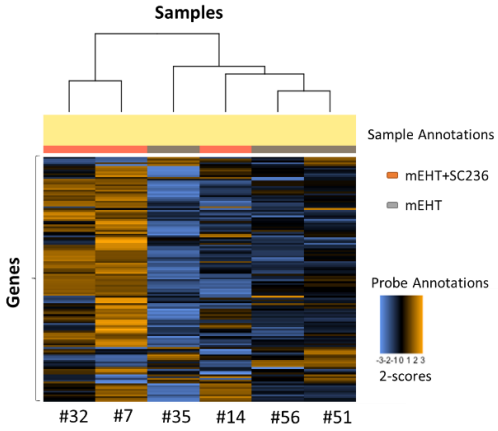

C

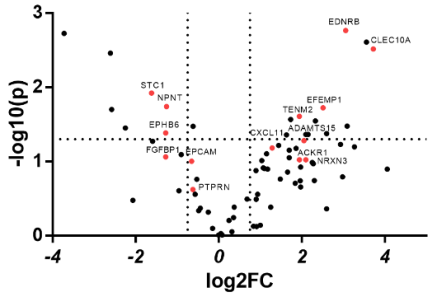

D

Term	Genes	Count	P value	Benjamini
Plasma membrane		7	3.60E-01	5.10E-01
Secreted proteins		6	4.50E-04	6.20E-03

Figure 14. Heat map and volcano plot of differentially expressed genes after modulated electro-hyperthermia (mEHT) vs mEHT+SC236 treatment from Nanostring data. (A) Experimental protocol. (B) Heat map of 74 differentially expressed genes (Nanostring nSolver® advanced analysis). Brown indicates upregulation, blue - downregulation. (C) - Volcano plot of the most differently expressed genes (significance levels are plotted against fold changes (FCs). Vertical dotted lines: $\log_2$ FC=0.75, horizontal dotted line: $-\log_{10}$(P) =1,30103. n=3/group. Genes marked with red dots are identified in Table 34(D) Regulated genes were clustered into two groups by DAVID. The Benjamini adjusted P-value indicates enrichment of genes in a particular functional category.

Upregulated proteins in mEHT+SC236 vs mEHT monotherapy were:

- A Disintegrin like And Metalloproteinase - with ThromboSpondin Type 1 motif 15 (ADAMTS15); C-X-C motif chemokine Ligand 11 (CXCL11); EGF -containing Fibulin -like Extracellular Matrix Protein (EFEMP1) which were identified by DAVID as secreted proteins.
- Atypical ChemoKine Receptor1 (ACKR1); TENeurin transmeMbrane protein 2 (TENM2); C-type LEctin domain Containing (CLEC10A); ENDothelin B Receptor (EDNRB); NeuReXiN protease -3 (NRXN3) which were identified by DAVID as membrane proteins.

Downregulated proteins were:

- Fibroblast Growth Factor-Binding Protein (FGFBP); NePhroNecTin (NPNT); STannioCalcin-1 (STC1) which were identified by DAVID as secreted proteins.
- EPithelial Cell Adhesion Molecule (EPCAM) and EPHrin type-B receptor 6 (EPHB6) which were identified by DAVID as membrane proteins.

Table 4. Absolute mRNA count of secreted and membrane proteins from the Nanostring data performed on the 4T1 cell line. Individual data of the mEHT and mEHT+SC236 group members and group averages. Bold indicates downregulation, non-bold-upregulation. Linear mRNA data was received through the nSolver advanced analysis method.

Group	**RNA count**	**mEHT**				**mEHT+SC236**			
	Genes	**#35**	**#51**	**#56**	**Avg.**	**#7**	**#14**	**#32**	**Avg.**
Secreted proteins	*Adamts15*	*28*	*98*	*74*	*65*	*294*	*286*	*113*	*231*
	Cxcl11	*77*	*89*	*148*	*105*	*370*	*213*	*396*	*326*
	Efemp1	*51*	*118*	*150*	*106*	*940*	*562*	*325*	*609*
	Fgfbp1	**355**	**224**	**155**	**245**	**56**	**174**	**68**	**99**
	Npnt	**1870**	**1714**	**817**	**1467**	**499**	**610**	**762**	**323**
	Stc1	**544**	**464**	**232**	**413**	**138**	**102**	**190**	**143**
Membrane proteins	*Ackr1*	*24*	*46*	*22*	*31*	*143*	*136*	*42*	*107*
	Tenm2	*3*	*19*	*19*	*14*	*47*	*87*	*35*	*56*
	Clec10a	*48*	*98*	*80*	*75*	*1239*	*1173*	*418*	*943*
	Ednrb	*48*	*62*	*51*	*54*	*614*	*352*	*231*	*399*
	Nrxn3	*4*	*10*	*11*	*9*	*27*	*40*	*22*	*29*
	Ephb6	**75**	**51**	**52**	**59**	**22**	**44**	**24**	**30**
	Epcam	**3263**	**5624**	**4580**	**4489**	**1832**	**3646**	**3090**	**2856**

5.7. Aspirin diminished lung nodules in the B16F10 melanoma model

In the melanoma tail vein injection model (Figure 15 A) pulmonary melanoma nodules were counted macroscopically. In untreated (Sham lungs 38.1 ± 16 nodules were counted. mEHT treatment alone reduced the number of nodules (28.8 ± 12) although the difference was not statistically significant However, mEHT combined with aspirin, significantly decreased the number of focies compared to mEHT alone (8.1 ± 8) (Figure 15 B, C). On the other hand, aspirin alone (31 ± 29) had no significant effect compared to Sham (26 ± 14) (Figure 15 D, E).

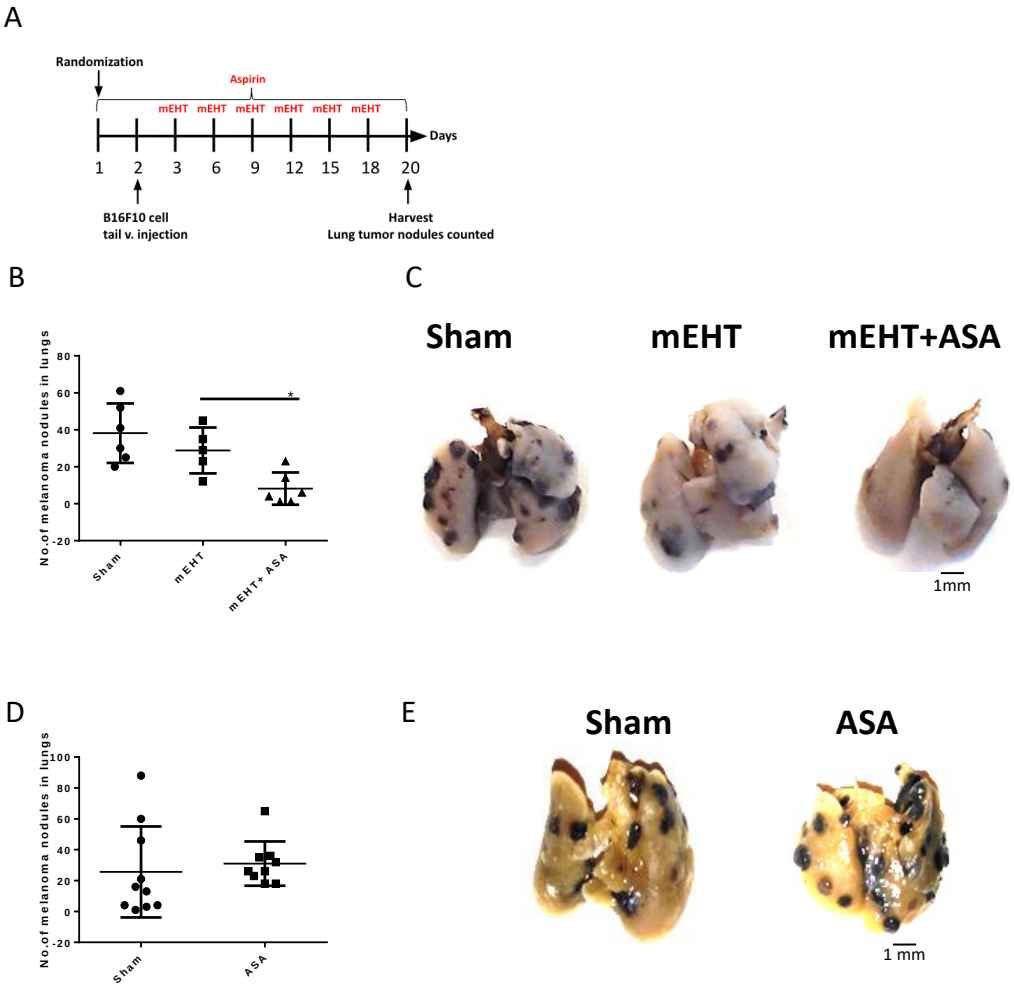

Figure 15. Effect of modulated electro-hyperthermia (mEHT) in combination with Aspirin on tumor burden in B16F10 mouse model. (A) Experimental protocol. (B) Quantification and (C) representative images of melanoma lung nodules in Sham, mEHT, and Aspirin + mEHT groups and in Sham and Aspirin groups (D, E). (Scale bar, 1 mm). Mean ± SEM, Unpaired Mann–Whitney test *: $p < 0.05$. Number of animals/groups: (B) Sham:6; mEHT:5; mEHT+ASA:6; (D) Sham:10; ASA:9.

6. Discussion

In the present study, we demonstrated that mEHT monotherapy induced inflammatory cytokines such as IL-6 and IL-1β. Inflammatory cytokines are a sign of more aggressive cancer phenotype [35,64]. By creating an inflammatory microenvironment within the tumor, IL-6 and IL-1β may promote tumor cell proliferation by activation of transcription factors and angiogenesis by the induction of key factors such as vascular endothelial growth factor (VEGF). There is a significant positive feedback loop between COX-2, IL-6, and IL-1β [59]. Based on the general knowledge, one of the COX-2 inducers are cytokines such as IL-1β [34] or IL-6 [49]. Our data revealed a COX-2 induction at 72- and 96-hours after mEHT treatment, which may be explained by the earlier upregulation of IL-6 and IL-1β at 12h and 24h. Similarly, to our results, a recent paper demonstrated relatively late COX-2 induction at 24h by chemotherapy (cisplatin and 5-FU) in 4T1 cells. Ablation of COX-2 with CRISPR/Cas9 effectively enhanced the treatment efficacy by reducing production of inflammatory proteins. Hence, similarly to our study, COX-2 inhibition was essential for effective combination therapy (chemo+immune therapy) [108]. Other studies demonstrated that photodynamic therapy has also induced significant IL-1β and COX-2 expression activating the tumor-favorable microenvironment, where COX-2 inhibitors were used to overcome the problem. A combination of photodynamic therapy with selective COX-2 inhibitors effectively inhibited inflammatory cytokine and VEGF synthesis and enhanced therapy-induced cytotoxicity and apoptosis [109].

In addition, CD105 (endoglin) was checked in time kinetics experiment, which represents the endothelial marker and is involved in the regulation of angiogenesis and wound healing [102]. We supposed significant blood vessel disruption after mEHT treatment at the 12h time point, which recovered over time. CD105 may represent a possible target combined with mEHT [102]. The concept related to blood vessel disruption after mEHT treatment was assessed by the study by our group Bokhari et al.2024 [110]. The study suggests that targeting angiogenesis and impairing tumor vascularization in combination with mEHT can synergistically inhibit tumor growth. This therapeutic strategy, however, requires further investigation.

In this hypothesis, it is suggested that NSAIDs may regulate the TME and mEHT-induced proinflammatory cytokines: IL-1β, IL-6, and COX-2. As a result, NSAIDs may enhance the mEHT-induced tumor cell death. Combining clinically available mEHT with NSAIDs is a new potential tool in oncologic therapy.

We combined mEHT with COX inhibitors, namely aspirin and SC-236 in TNBC 4T1 and B16F10 melanoma experimental mouse models. The 4T1 TNBC growth inhibitory effect of mEHT monotherapy was quite similar to our previously published studies, where mEHT alone effectively inhibited 4T1 TNBC growth after the third treatment [18,19]. However, here the combination of mEHT with NSAIDs, demonstrated significant tumor shrinkage earlier: already after the second treatment, as revealed by both ultrasound and a digital caliper measurements of tumor volume. The clinical relevance of achieving tumor reduction at an earlier stage of treatment is enormous, as earlier inhibition of exponential tumor growth offers better prognosis. Shrinking the tumor early, may render it more susceptible to subsequent treatments like surgery, radiation, or chemotherapy. Thus, early tumor size reduction could potentially make these treatments more effective, leading to better outcomes [111]. Early cancer treatment is also emphasized by the recent NHS cancer guideline[112]. The tumor volume proved to be markedly small after combined treatment (mEHT+SC236) only after the fourth treatment compared to mEHT.

Besides the tumor size reduction in the NSAID combined groups the tumor destruction ratio (TDR) of the remaining small tumors was also larger. However, in mEHT- monotherapy treated tumors, only tumor size was smaller than in the Sham-treated tumors. The TDR did not differ significantly, similarly to our previous studies [18]. The lack of significant increase in TDR is largely due to the severe spontaneous destruction of Sham tumors growing to a size where spontaneous necrosis is evident [113].

Moreover, the tumor damage response was accompanied by a significant increase in cleaved caspase 3, suggesting that apoptosis played an important role in the antitumor effect of mEHT and NSAIDs [114]. As cancer cells often evade apoptosis, inducing apoptosis in cancer cells is a critical goal of cancer treatment. The intrinsic resistance of cancer cells to apoptosis is the basis of resistance to chemotherapy [115]. Thus, induction or reactivation of

apoptosis in cancer sensitizes cancer cells to therapy [116]. Monotherapy with both mEHT or COX-2 inhibitors induced significant cC3 staining in TNBC in the previous [19,117],as well as in this present study. COX-2 inhibition and mEHT-induced apoptosis may have contributed to the synergistic effects of mEHT+NSAIDs [70,118].

Non-steroid anti-inflammatory drugs have never been used in combination with mEHT before us. Although, a natural agent like curcumin, has similar anti-inflammatory properties. Indeed, by attenuating M2 TAM and MDSC tumour infiltration on CT26 colon cancer mouse model, curcumin effectively synergized mEHT-mediated tumor growth suppression [119].

Neither mEHT, nor the NSAIDs, nor any combination appeared to be toxic based on the body weight data as animals did not lose more than 5-10% of their body weight [47]. Assessing treatment toxicity in preclinical models is crucial to evaluate the safety for clinical translation [2]. Based on the body surface area dose conversion method [120], 100 mg/kg ASA is equivalent to a moderate human ASA dose of 300-500 mg/day [81]. Long-term ASA treatment can result in renal, cardiovascular, and gastric toxicity as well as bleeding and hypersensitivity [121]. SC236 used in the present study is analogous to Celecoxib. Celecoxib is associated with a decreased risk of gastrointestinal bleeding, although it still has a higher incidence of cardiovascular events in comparison to traditional NSAIDs [122]. Although the applied mEHT+NSAID dose combination did not appear to have any toxicity, the toxicity findings of the present mouse study must be reevaluated in large animal models and early-phase clinical studies before reaching conclusions relevant to the clinical setting.

According to our RT-qPCR data NSAIDs attenuated mEHT induced IL-1β and COX-2 expression. Besides inflammatory proteins, NSAIDs may affect COX-independent inflammatory pathways, by the inhibition pathways that support cell proliferation and angiogenesis but suppress apoptosis [76–79]. Therefore, COX inhibition-induced apoptosis sensitizes cancer to other conventional anti-cancer therapies such as chemotherapy, immunotherapy, radiotherapy [85,86] or mEHT [123].

The results of the Nanostring multiplex data analysis demonstrated that the combination of mEHT with a selective COX-2 inhibitor regulated secreted and cell

membrane proteins. Some of the secreted proteins are extracellular matrix (ECM) proteins (EFEMP1, NPNT, STC), ECM regulators (ADAMTS15, CXCL11, FGFBP1,) and thus are an essential part of the tumor microenvironment. The identified membrane proteins serve as receptors (EPHB6, ACKR1, EDNRB) or adhesion molecules (EPCAM) and may enhance antitumor immunity (TENM2 and CLEC-10A), thus they may contributed enhanced mEHT induced cancer destruction through regulating the TME related immune response.

ADAMTS15 was upregulated in mEHT+ SC236 compared to mEHT monotherapy. It is involved in extracellular matrix remodeling [124,125], and participates in tissue organization and vascular homeostasis. ADAMTS15 is a secreted protease modifying the extracellular matrix components like proteoglycans and collagen [126]. The role of ADAMTS15 in tumor pathophysiology is inhibition of angiogenesis and cell migration [127]. To our knowledge, the regulation of ADAMTS15 by COX-2 has not been described before. ADAMTS15 may be acting as a tumor suppressor in breast cancer by modulating cell-environment interactions [128,129]. ADAMTS15 expression is a favorable prognostic factor in breast cancer. Higher expression has been associated with better clinical outcomes, including longer overall survival and disease-free survival [130] [131].

Similarly, secreted proteins, such as EFEMP1 and CXCL11, which are known targets of selCOXIBs [46], were also upregulated in the combination group. EFEMP1 is an extracellular matrix protein, associated with elastic fiber formation and cell adhesion [132] and is considered a tumor-suppressor gene [133,134]. Its expression is diminished in breast cancer [135]. The anti-angiogenic properties (reduction of angiogenic sprouting) of EFEMP1 have been described [136]. Although contradictory data suggesting EFEMP1 to be a bad prognostic indicator have been also published [137], our data support the beneficial role of EFEMP1 in breast cancer. CXCL11 is involved in the immune response including T-cell and TME regulation. CXCL11 can enhance antitumor immune cell migration and infiltration in the breast cancer tissue [138].

Additionally, downregulated secreted glycoproteins were FGFBP1, STC1 and NPNT. FGFBP1's physiologic role is to regulate fibroblasts and some cellular processes, such as differentiation and growth. In cancer biology, FGFBP1 may stimulate angiogenesis, PD-L1

expression and immune inhibition [139,140]. STC1 is a secreted glycoprotein. Its biological role is the regulation of phosphate and calcium homeostasis [141]. In cancer cells, STC1 enhances metastasis via the PI-3K/Akt/NF-κB signaling pathways [142]. Similarly to our results, a study demonstrated, that NSAIDs (Ibuprofen) attenuated IL-1β induced STC1 expression in chondrocytes [143]. The glycoprotein NPNT is secreted into the TNBC extracellular matrix and plays a role in adhesion and migration. In cancer, NPNT may promote metastasis via its integrin-binding site, which is important for adhesion and transmigration through the endothelial cells [144]. Thus, downregulation of NPNT by NSAIDs may have contributed to the reduced tumor formation in our lung melanoma model. Regulation of NPNT and FGFBP1 by COX-inhibition has not been described before. As described, FGFBP1, STC1 and NPNT proteins have tumor promoting effect, thus, downregulation of these proteins could have contributed to the synergistic effect seen in our study.

Membrane glycoproteins, such as ACKR1, EDNRB, TENM2 and CLEC-10A, were highly expressed in the selCoxib treated group. These proteins are considered as biomarkers of good prognosis for various cancers. They may negatively regulate the tumor-favorable microenvironment and support the anti-tumor immunity in breast cancer, although their role in tumor pathophysiology is not yet completely understood [145–148]. The regulation of these proteins by COX-inhibition has not been described before. In our study, the upregulation of these proteins by selCoxIb treatment probably contributed to the enhanced effects of mEHT in treating tumors. Neurexin 3 (NRXN3) encodes a protein involved in synaptic signaling and neural development in the nervous system [149]. Overlaps between genes involved in neural development and in cancer, suggest links between nervous system development and tumorigenesis [150,151]. Emerging research suggests a role of NRXN3 in some cancers, including breast cancer [152], through its involvement in cellular adhesion, migration, and invasion.

Additionally, the expression of the membrane proteins EPCAM and EPHB6 were downregulated by selCoxib treatment. Their biological role has been associated with cell-adhesion and signaling. Thus, they may stimulate 4T1 cell growth, therefore, EPCAM and

EPHB6 are associated with poor survival [153]. Silencing EPCAM significantly decreased the capacity of TNBC cell proliferation [154]. EPCAM expression is related to COX-2 expression, TME regulation, and angiogenesis [155].

The listed regulated genes are mostly considered predictor biomarkers of prognosis in various cancers. The clinical implications of these genes are often context-dependent, and continuous research is essential to comprehend their roles in diseases and how they can be utilized for clinical purposes like diagnosis, prognosis, and targeted therapies.

Furthermore, we investigated the combination therapy of mEHT with aspirin in the B16F10 melanoma model. Tumor nodules in the lungs were targeted with a new application method developed by Thomas MJ et al in 2020 [105]. The pulmonary nodules were counted to evaluate the effect of the combination therapy. Our findings suggest, that mEHT efficacy was enhanced by aspirin, however, aspirin alone did not reduce the nodule count in the lungs. The study has shown the positive impact of aspirin in the B16F10 tumor model, as it induces cC3-mediated apoptosis. [83,106]. Our data in 4T1 TNBC model also supports the role of cC3-mediated apoptosis. It appears that cC3-mediated apoptosis might contribute to the observed synergistic inhibition of tumor growth [34], [35]. Although, the exact molecular mechanism needs to be further investigated.

7. Conclusion

We suggest a new combination treatment protocol, which could be implicated in the clinical setting as a therapeutic option due to its effectiveness and availability.

We can draw the following conclusion based on our results:

1. mEHT treatment stimulated the expression of proinflammatory cytokines IL-1β, IL-6, and COX-2 in 4T1 TNBC
2. The combination therapy of mEHT+aspirin and mEHT+SC236 demonstrated a synergistic inhibition of tumor growth in 4T1 TNBC animal cancer model. However, selective COX-2 inhibition proved to be more effective
3. The mEHT induced expression of IL-1β and COX-2 were attenuated after COX-2 inhibition
4. Selective COX-2 inhibition enhanced mEHT-induced tumor destruction
5. Selective COX-2 inhibition may modulate the extracellular matrix, and cell membrane functions in the tumor microenvironment leading to inhibition of cancer cell proliferation
6. Apirin+mEHT demonstrated synergistic lung nodule inhibition in B16F10 melanoma mouse model

8. Summary

Triple-negative breast cancer (TNBC) is a leading cause of cancer mortality and lacks modern therapy options. Modulated electro-hyperthermia (mEHT) is an adjuvant therapy which demonstrated clinical efficacy for the treatment of various cancer types. In this study, we report that mEHT monotherapy stimulated interleukin-1 beta (IL-1β) and interleukin-6 (IL-6) expression, and consequently cyclooxygenase 2 (COX-2), which may favor a cancer-promoting tumor microenvironment. Thus, we combined mEHT with non-steroid anti-inflammatory drugs (NSAIDs): a non-selective aspirin, or the selective COX-2 inhibitor SC236, *in vivo*. We demonstrate that NSAIDs synergistically increased the tumor growth antagonizing effect of mEHT in the 4T1 TNBC model. Moreover, the strongest tumor destruction ratio (TDR) was observed mEHT was applied with the the combination of SC236. IL-1β and COX-2 expression were significantly reduced by the combination therapies. Furthermore, tumor damage was accompanied by a significant increase in cleaved caspase-3 (cC3), suggesting that apoptosis played an important role. Additionally, a custom-made Nanostring panel demonstrated significant upregulation of genes participating in the formation of the extracellular matrix and cell membrane functions. Similarly, in the B16F10 melanoma model, mEHT and aspirin synergistically reduced the number of melanoma nodules in the lungs. In conclusion, mEHT combined with selective COX-2 inhibitors may offer a new therapeutic option in the treatment of TNBC.

9. References

1. Lee SY, Lorant G, Grand L, Szasz AM. The Clinical Validation of Modulated Electro-Hyperthermia (mEHT). Vol. 15, Cancers. Multidisciplinary Digital Publishing Institute (MDPI); 2023.

2. Mak IW, Evaniew N, Ghert M. Review Article Lost in translation: animal models and clinical trials in cancer treatment. Vol. 6, Am J Transl Res. 2014. Available from: www.ajtr.org

3. Alshaibi HF, Al-Shehri B, Hassan B, Al-Zahrani R, Assiss T. Modulated Electrohyperthermia: A New Hope for Cancer Patients. Vol. 2020, BioMed Research International. Hindawi Limited; 2020.

4. Tsang YW, Chi KH, Huang CC, Chi MS, Chiang HC, Yang KL, Li WT, Wang YS. Modulated electro-hyperthermia-enhanced liposomal drug uptake by cancer cells. Int J Nanomedicine. 2019;14:1269–1279.

5. Qin W, Akutsu Y, Andocs G, Suganami A, Hu X, Yusup G, Komatsu-Akimoto A, Hoshino I, Hanari N, Mori M, Isozaki Y, Akanuma N, Tamura Y, Matsubara H. Modulated electro-hyperthermia enhances dendritic cell therapy through an abscopal effect in mice. Oncol Rep. 2014 Dec 1;32(6):2373–2379.

6. Bodis S, Baranowska-Kortylewicz J, Cappabianca S, Szasz A. Heterogeneous Heat Absorption Is Complementary to Radiotherapy. 2022; Available from: https://doi.org/10.3390/cancers14040901

7. McDonald M, Corde S, Lerch M, Rosenfeld A, Jackson M, Tehei M. First in vitro evidence of modulated electro-hyperthermia treatment performance in combination with megavoltage radiation by clonogenic assay. Sci Rep. 2018 Dec 1;8(1).

8. Minnaar CA, Kotzen JA. Modulated electro hyperthermia as an immune modulator with checkpoint inhibitors and radiotherapy. Eur J Cancer. 2019 Mar 1;110:S19–20. Available from: https://doi.org/10.1016/j.ejca.2019.01.068

9. Krenacs T, Meggyeshazi N, Forika G, Kiss E, Hamar P, Szekely T, Vancsik T. Modulated electro-hyperthermia-induced tumor damage mechanisms revealed in cancer models. Int J Mol Sci. 2020 Sep 1;21(17):1–25.

10. Szász A, Schweitzer S, Schulz I, Balogh V, Herzog A, K Pang CL, Douwes F, Hegyi G, Marcell Szász habil A, Parmar G, Kwan-Hwa C, Yu-Shan Wang S. Editor-in-Chief Managing Editors Editorial Board Balázs Tóth. Oncothermia Journal, Special Edition. 2020. Available from: https://www.cambridgescholars.com/challenges-and-

11. Muftuler LT, Hamamura MJ, Birgul O, Nalcioglu O. In vivo MRI electrical impedance tomography (MREIT) of tumors. Technology in cancer research & treatment. 2006 Aug;5(4):381—387. Available from: http://europepmc.org/abstract/MED/16866568

12. Kao PHJ, Chen CH, Tsang YW, Lin CS, Chiang HC, Huang CC, Chi MS, Yang KL, Li WT, Kao SJ, Minnaar CA, Chi KH, Wang YS. Relationship between Energy Dosage and Apoptotic Cell Death by Modulated Electro-Hyperthermia. Sci Rep. 2020 Dec 1;10(1).

13. Krenacs T, Meggyeshazi N, Forika G, Kiss E, Hamar P, Szekely T, Vancsik T. Modulated electro-hyperthermia-induced tumor damage mechanisms revealed in cancer models. Int J Mol Sci. 2020 Sep 1;21(17):1–25.

14. Szasz AM, Minnaar CA, Szentmártoni G, Szigeti GP, Dank M. Review of the Clinical Evidences of Modulated Electro-Hyperthermia (mEHT) Method: An Update for the Practicing Oncologist. Vol. 9, Frontiers in Oncology. Frontiers Media S.A.; 2019.

15. Wismeth C, Dudel C, Pascher C, Ramm P, Pietsch T, Hirschmann B, Reinert C, Proescholdt M, Rümmele P, Schuierer G, Bogdahn U, Hau P. Transcranial electro-hyperthermia combined with alkylating chemotherapy in patients with relapsed high-grade gliomas: Phase i clinical results. J Neurooncol. 2010 Jul;98(3):395–405.

16. Nagata T, Kanamori M, Sekine S, Arai M, Moriyama M, Fujii T. Clinical study of modulated electro-hyperthermia for advanced metastatic breast cancer. Mol Clin Oncol. 2021;14(5).

17. Minnaar CA, Kotzen JA, Ayeni OA, Naidoo T, Tunmer M, Sharma V, Vangu MDT, Baeyens A. The effect of modulated electro-hyperthermia on local disease control in HIV-positive and -negative cervical cancer women in South Africa: Early results from a phase III randomised controlled trial. PLoS One. 2019 Jun 1;14(6).

18. Schvarcz CA, Danics L, Krenács T, Viana P, Béres R, Vancsik T, Nagy Á, Gyenesei A, Kun J, Fonović M, Vidmar R, Benyó Z, Kaucsár T, Hamar P. Modulated electro-hyperthermia induces a prominent local stress response and growth inhibition in mouse breast cancer isografts. Cancers (Basel). 2021 Apr 1;13(7).

19. Danics L, Schvarcz CA, Viana P, Vancsik T, Krenács T, Benyó Z, Kaucsár T, Hamar P. Exhaustion of protective heat shock response induces significant tumor damage by apoptosis after modulated electro-hyperthermia treatment of triple negative breast cancer isografts in mice. Cancers (Basel). 2020 Sep 1;12(9):1–24.

20. Zagami P, Carey LA. Triple negative breast cancer: Pitfalls and progress. NPJ Breast Cancer. 2022;8(1):95. Available from: https://doi.org/10.1038/s41523-022-00468-0

21. Akshata Desai KA. Triple Negative Breast Cancer – An Overview. Hereditary Genetics. 2012;

22. Obidiro O, Battogtokh G, Akala EO. Triple Negative Breast Cancer Treatment Options and Limitations: Future Outlook. Vol. 15, Pharmaceutics. Multidisciplinary Digital Publishing Institute (MDPI); 2023.

23. Li Y, Zhang H, Merkher Y, Chen L, Liu N, Leonov S, Chen Y. Recent advances in therapeutic strategies for triple-negative breast cancer. J Hematol Oncol. 2022;15(1):121. Available from: https://doi.org/10.1186/s13045-022-01341-0

24. Wahba HA, El-Hadaad HA. Current approaches in treatment of triple-negative breast cancer. Vol. 12, Cancer Biology and Medicine. Cancer Biology and Medicine; 2015. p. 106–116.

25. Yin L, Duan JJ, Bian XW, Yu SC. Triple-negative breast cancer molecular subtyping and treatment progress. Vol. 22, Breast Cancer Research. BioMed Central Ltd; 2020.

26. Chattopadhyay C, Kim DW, Gombos DS, Oba J, Qin Y, Williams MD, Esmaeli B, Grimm EA, Wargo JA, Woodman SE, Patel SP. Uveal melanoma: From diagnosis to treatment and the science in between. Vol. 122, Cancer. John Wiley and Sons Inc.; 2016. p. 2299–2312.

27. Pavri SN, Clune J, Ariyan S, Narayan D. Malignant Melanoma: Beyond the Basics. Plast Reconstr Surg. 2016;138(2). Available from: https://journals.lww.com/plasreconsurg/fulltext/2016/08000/malignant_melanoma__beyond_the_basics.42.aspx

28. Knackstedt T, Knackstedt RW, Couto R, Gastman B. Malignant Melanoma: Diagnostic and Management Update. Plast Reconstr Surg. 2018;142(2). Available from: https://journals.lww.com/plasreconsurg/fulltext/2018/08000/malignant_melanoma__diagnostic_and_management.38.aspx

29. Sood S, Jayachandiran R, Pandey S. Current Advancements and Novel Strategies in the Treatment of Metastatic Melanoma. Vol. 20, Integrative Cancer Therapies. SAGE Publications Inc.; 2021.

30. Rothermel LD, Sarnaik AA, Khushalani NI, Sondak VK. Current Immunotherapy Practices in Melanoma. Vol. 28, Surgical Oncology Clinics of North America. W.B. Saunders; 2019. p. 403–418.

31. Leonardi GC, Falzone L, Salemi R, Zanghì A, Spandidos DA, Mccubrey JA, Candido S, Libra M. Cutaneous melanoma: From pathogenesis to therapy (Review). Vol. 52, International Journal of Oncology. Spandidos Publications; 2018. p. 1071–1080.

32. Rouzer CA, Marnett LJ. Structural and Chemical Biology of the Interaction of Cyclooxygenase with Substrates and Non-Steroidal Anti-Inflammatory Drugs. Vol. 120, Chemical Reviews. American Chemical Society; 2020. p. 7592–7641.

33. Smith WL, Dewitt DL, Garavito RM. CYCLOOXYGENASES: Structural, Cellular, and Molecular Biology. 2000

34. Crofford LJ, Wilder RL, Ristimaki AP, Sano H, Remmers EF, Epps HR, Hla T. Cyclooxygenase-1 and-2 Expression in Rheumatoid Synovial Tissues Effects of Interleukin-1f, Phorbol Ester, and Corticosteroids.

35. Dossus L, Kaaks R, Canzian F, Albanes D, Berndt SI, Boeing H, Buring J, Chanock SJ, Clavel-Chapelon F, Feigelson HS, Gaziano JM, Giovannucci E, Gonzalez C, Haiman CA, Hallmans G, Hankinson SE, Hayes RB, Henderson BE, Hoover RN, Hunter DJ, Khaw KT, Kolonel LN, Kraft P, Ma J, Le Marchand L, Lund E, Peeters PHM, Stampfer M, Stram DO, Thomas G, Thun MJ, Tjonneland A, Trichopoulos D, Tumino R, Riboli E, Virtamo J, Weinstein SJ, Yeager M, Ziegler RG, Cox DG. PTGS2 and IL6 genetic variation and risk of breast and prostate cancer: Results from the Breast and Prostate Cancer Cohort Consortium (BPC3). Carcinogenesis. 2010 Mar;31(3):455–461.

36. Hwang D, Scollard D, Byrne J, Levine E. Expression of Cyclooxygenase-1 and Cyclooxygenase-2 in Human Breast Cancer. Available from: https://academic.oup.com/jnci/article/90/6/455/887943

37. Sezgin Alikanoglu A, Kaya V. Expression of cyclooxygenase-2 and Bcl-2 in breast cancer and their relationship with triple-negative disease. Available from: www.jbuon.com

38. Lin F, Luo J, Gao W, Wu J, Shao Z, Wang Z, Meng J, Ou Z, Yang G. COX-2 promotes breast cancer cell radioresistance via p38/MAPK-mediated cellular anti-apoptosis and invasiveness. Tumor Biology. 2013 Oct 1;34(5):2817–2826.

39. Hosseini F, Mahdian-Shakib A, Jadidi-Niaragh F, Enderami SE, Mohammadi H, Hemmatzadeh M, Mohammed HA, Anissian A, Kokhaei P, Mirshafiey A, Hassannia H. Anti-inflammatory and anti-tumor effects of α-L-guluronic acid (G2013) on cancer-related inflammation in a murine breast cancer model. Biomedicine and Pharmacotherapy. 2018 Feb 1;98:793–800.

40. Menter DG, DuBois RN. Prostaglandins in Cancer Cell Adhesion, Migration, and Invasion. Oh ES, editor. Int J Cell Biol. 2012;2012:723419. Available from: https://doi.org/10.1155/2012/723419

41. Todoric J, Antonucci L, Karin M. Targeting inflammation in cancer prevention and therapy. Vol. 9, Cancer Prevention Research. American Association for Cancer Research Inc.; 2016. p. 895–905.

42. Hsieh CC, Wang CH. Aspirin Disrupts the Crosstalk of Angiogenic and Inflammatory Cytokines between 4T1 Breast Cancer Cells and Macrophages. 2018; Available from: https://doi.org/10.1155/2018/6380643

43. Hsieh CC, Huang YS. Aspirin breaks the crosstalk between 3T3-L1 adipocytes and 4T1 breast cancer cells by regulating cytokine production. PLoS One. 2016 Jan 1;11(1).

44. Rummel C, Sachot C, Poole S, Luheshi GN. Circulating interleukin-6 induces fever through a STAT3-linked activation of COX-2 in the brain. Am J Physiol Regul Integr Comp Physiol. 2006;291:1316–26. Available from: http://www.ajpregu.org

45. Gilligan MM, Gartung A, Sulciner ML, Norris PC, Sukhatme VP, Bielenberg DR, Huang S, Kieran MW, Serhan CN, Panigrahy D. Aspirin-triggered proresolving mediators stimulate resolution in cancer. Proc Natl Acad Sci U S A. 2019;116(13):6292–6307.

46. Zelenay S, Van Der Veen AG, Böttcher JP, Snelgrove KJ, Rogers N, Acton SE, Chakravarty P, Girotti MR, Marais R, Quezada SA, Sahai E, Reis E Sousa C.

Cyclooxygenase-Dependent Tumor Growth through Evasion of Immunity. Cell. 2015 Oct 28;162(6):1257–1270.

47. Xu L, Stevens J, Hilton MB, Seaman S, Conrads TP, Veenstra TD, Logsdon D, Morris H, Swing DA, Patel NL, Kalen J, Haines DC, Zudaire E, St Croix B. COX-2 inhibition potentiates antiangiogenic cancer therapy and prevents metastasis in preclinical models. Sci Transl Med. 2014 Jun 25;6(242).

48. Chen EP, Smyth EM. COX-2 and PGE 2-dependent immunomodulation in breast cancer. 2011;

49. Sorli CH, Zhang HJ, Armstrong MB, Rajotte R V, Maclouf J, Paul Robertson R. Basal expression of cyclooxygenase-2 and nuclear factor-interleukin 6 are dominant and coordinately regulated by interleukin 1 in the pancreatic islet. Vol. 95, Medical Sciences Communicated by Donald C. Malins, Pacific Northwest Research Foundation. 1998. Available from: www.pnas.org.

50. Sinha P, Clements VK, Fulton AM, Ostrand-Rosenberg S. Prostaglandin E2 promotes tumor progression by inducing myeloid-derived suppressor cells. Cancer Res. 2007 May 1;67(9):4507–2513.

51. Hong DS, Angelo LS, Kurzrock R. Interleukin-6 and its receptor in cancer: Implications for translational therapeutics. Vol. 110, Cancer. 2007. p. 1911–1928.

52. Diederich M, Sobolewski C, Cerella C, Dicato M, Ghibelli L. The role of cyclooxygenase-2 in cell proliferation and cell death in human malignancies. International Journal of Cell Biology. 2010.

53. Bell CR, Pelly VS, Moeini A, Chiang SC, Flanagan E, Bromley CP, Clark C, Earnshaw CH, Koufaki MA, Bonavita E, Zelenay S. Chemotherapy-induced COX-2 upregulation by cancer cells defines their inflammatory properties and limits the efficacy of chemoimmunotherapy combinations. Nat Commun. 2022 Dec 1;13(1).

54. Huang Q, Li F, Liu X, Li W, Shi W, Liu FF, O'Sullivan B, He Z, Peng Y, Tan AC, Zhou L, Shen J, Han G, Wang XJ, Thorburn J, Thorburn A, Jimeno A, Raben D,

Bedford JS, Li CY. Caspase 3-mediated stimulation of tumor cell repopulation during cancer radiotherapy. Nat Med. 2011 Jul;17(7):860–866.

55. Chai Y, Calaf GM, Zhou H, Ghandhi SA, Elliston CD, Wen G, Nohmi T, Amundson SA, Hei TK. Radiation induced COX-2 expression and mutagenesis at non-targeted lung tissues of gpt delta transgenic mice. Br J Cancer. 2013 Jan 15;108(1):91–98.

56. Alvarez AM, DeOcesano-Pereira C, Teixeira C, Moreira V. IL-1β and TNF-α Modulation of Proliferated and Committed Myoblasts: IL-6 and COX-2-Derived Prostaglandins as Key Actors in the Mechanisms Involved. Cells. 2020 Sep 1;9(9).

57. Zhang Q, Zhu B, Li Y. Resolution of cancer-promoting inflammation: A new approach for anticancer therapy. Vol. 8, Frontiers in Immunology. Frontiers Research Foundation; 2017.

58. Zhang JM, An J. Cytokines, inflammation, and pain. Vol. 45, International Anesthesiology Clinics. 2007. p. 27–37.

59. Neeb L, Hellen P, Boehnke C, Hoffmann J, Schuh-Hofer S, Dirnagl U, Reuter U. IL-1β stimulates COX-2 dependent PGE2 synthesis and CGRP release in rat trigeminal ganglia cells. PLoS One. 2011;6(3).

60. Xu J, Ye Y, Zhang H, Szmitkowski M, Mäkinen MJ, Li P, Xia D, Yang J, Wu Y, Wu H. Diagnostic and prognostic value of serum interleukin-6 in colorectal cancer. Medicine (United States). 2016 Jan 1;95(2).

61. Gao SP, Mark KG, Leslie K, Pao W, Motoi N, Gerald WL, Travis WD, Bornmann W, Veach D, Clarkson B, Bromberg JF. Mutations in the EGFR kinase domain mediate STAT3 activation via IL-6 production in human lung adenocarcinomas. Journal of Clinical Investigation. 2007 Dec;117(12):3846–3856.

62. Bent R, Moll L, Grabbe S, Bros M. Interleukin-1 beta—A friend or foe in malignancies? Vol. 19, International Journal of Molecular Sciences. MDPI AG; 2018.

63. Gelfo V, Romaniello D, Mazzeschi M, Sgarzi M, Grilli G, Morselli A, Manzan B, Rihawi K, Lauriola M. Roles of il-1 in cancer: From tumor progression to resistance to targeted therapies. Vol. 21, International Journal of Molecular Sciences. MDPI AG; 2020. p. 1–14.

64. Esquivel-Velázquez M, Ostoa-Saloma P, Palacios-Arreola MI, Nava-Castro KE, Castro JI, Morales-Montor J. The role of cytokines in breast cancer development and progression. Vol. 35, Journal of Interferon and Cytokine Research. Mary Ann Liebert Inc.; 2015. p. 1–16.

65. Wang B, Wu L, Chen J, Dong L, Chen C, Wen Z, Hu J, Fleming I, Wang DW. Metabolism pathways of arachidonic acids: mechanisms and potential therapeutic targets. Vol. 6, Signal Transduction and Targeted Therapy. Springer Nature; 2021.

66. Zappavigna S, Cossu AM, Grimaldi A, Bocchetti M, Ferraro GA, Nicoletti GF, Filosa R, Caraglia M. Anti-inflammatory drugs as anticancer agents. Int J Mol Sci. 2020 Apr 1;21(7).

67. Rouzer CA, Marnett LJ. Structural and Chemical Biology of the Interaction of Cyclooxygenase with Substrates and Non-Steroidal Anti-Inflammatory Drugs. Vol. 120, Chemical Reviews. American Chemical Society; 2020. p. 7592–7641.

68. Bindu S, Mazumder S, Bandyopadhyay U. Non-steroidal anti-inflammatory drugs (NSAIDs) and organ damage: A current perspective. Vol. 180, Biochemical Pharmacology. Elsevier Inc.; 2020.

69. Curtis E, Fuggle N, Shaw S, Spooner L, Ntani G, Parsons C, Corp N, Honvo G, Baird J, Maggi S, Dennison E, Bruyère O, Reginster JY, Cooper C. Safety of Cyclooxygenase-2 Inhibitors in Osteoarthritis: Outcomes of a Systematic Review and Meta-Analysis. Vol. 36, Drugs and Aging. Springer International Publishing; 2019. p. 25–44.

70. Kolawole OR, Kashfi K. NSAIDs and Cancer Resolution: New Paradigms beyond Cyclooxygenase. Vol. 23, International Journal of Molecular Sciences. MDPI; 2022.

71. Gamba CA, Swetter SM, Stefanick ML, Kubo J, Desai M, Spaunhurst KM, Sinha AA, Asgari MM, Sturgeon S, Tang JY. Aspirin is associated with lower melanoma risk among postmenopausal Caucasian women: The Women's Health Initiative. Cancer. 2013 Apr 15;119(8):1562–1609.

72. Bardia A, Keenan TE, Ebbert JO, Lazovich D, Wang AH, Vierkant RA, Olson JE, Vachon CM, Limburg PJ, Anderson KE, Cerhan JR. Personalizing Aspirin Use for Targeted Breast Cancer Chemoprevention in Postmenopausal Women. Mayo Clin Proc. 2016 Jan 1;91(1):71–80.

73. Ashok V, Dash C, Rohan TE, Sprafka JM, Terry PD. Selective cyclooxygenase-2 (COX-2) inhibitors and breast cancer risk. Breast. 2011;20(1):66–70.

74. Díaz-González F, Sánchez-Madrid F. NSAIDs: Learning new tricks from old drugs. Eur J Immunol. 2015 Mar 1;45(3):679–686.

75. Pu D, Yin L, Huang L, Qin C, Zhou Y, Wu Q, Li Y, Zhou Q, Li L. Cyclooxygenase-2 Inhibitor: A Potential Combination Strategy With Immunotherapy in Cancer. Vol. 11, Frontiers in Oncology. Frontiers Media S.A.; 2021.

76. Park MH, Hong JT. Roles of NF-κB in cancer and inflammatory diseases and their therapeutic approaches. Vol. 5, Cells. MDPI; 2016.

77. Setia S, Nehru B, Sanyal SN. Upregulation of MAPK/Erk and PI3K/Akt pathways in ulcerative colitis-associated colon cancer. Biomedicine and Pharmacotherapy. 2014 Oct 1;68(8):1023–1029.

78. Zhang P, He D, Song E, Jiang M, Song Y. Celecoxib enhances the sensitivity of nonsmall- cell lung cancer cells to radiationinduced apoptosis through downregulation of the Akt/mTOR signaling pathway and COX-2 expression. PLoS One. 2019 Oct 1;14(10).

79. Benelli R, Barboro P, Costa D, Astigiano S, Barbieri O, Capaia M, Poggi A, Ferrari N. Multifocal signal modulation therapy by celecoxib: A strategy for managing castration-resistant prostate cancer. Int J Mol Sci. 2019 Dec 1;20(23).

80. Huang C, Chen Y, Liu H, Yang J, Song X, Zhao J, He N, Zhou CJ, Wang Y, Huang C, Dong Q. Celecoxib targets breast cancer stem cells by inhibiting the synthesis of prostaglandin E 2 and down-regulating the Wnt pathway activity. 2017. Available from: www.impactjournals.com/oncotarget

81. Maity G, De A, Das A, Banerjee S, Sarkar S, Banerjee SK. Aspirin blocks growth of breast tumor cells and tumor-initiating cells and induces reprogramming factors of mesenchymal to epithelial transition. Laboratory Investigation. 2015 Jul 27;95(7):702–717.

82. Roche-Nagle G, Connolly EM, Eng M, Bouchier-Hayes DJ, Harmey JH. Antimetastatic activity of a cyclooxygenase-2 inhibitor. Br J Cancer. 2004 Jul 19;91(2):359–365.

83. Lucotti S, Cerutti C, Soyer M, Gil-Bernabé AM, Gomes AL, Allen PD, Smart S, Markelc B, Watson K, Armstrong PC, Mitchell JA, Warner TD, Ridley AJ, Muschel RJ. Aspirin blocks formation of metastatic intravascular niches by inhibiting platelet-derived COX-1/ thromboxane A2. Journal of Clinical Investigation. 2019 May 1;129(5):1845–1862.

84. Xu L, Stevens J, Hilton MB, Seaman S, Conrads TP, Veenstra TD, Logsdon D, Morris H, Swing DA, Patel NL, Kalen J, Haines DC, Zudaire E, St Croix B. COX-2 inhibition potentiates antiangiogenic cancer therapy and prevents metastasis in preclinical models. Sci Transl Med. 2014 Jun 25;6(242).

85. Ramos-Inza S, Ruberte AC, Sanmartín C, Sharma AK, Plano D. NSAIDs: Old Acquaintance in the Pipeline for Cancer Treatment and Prevention-Structural Modulation, Mechanisms of Action, and Bright Future. Vol. 64, Journal of Medicinal Chemistry. American Chemical Society; 2021. p. 16380–16421.

86. Connolly EM, Harmey JH, O'Grady T, Foley D, Roche-Nagle G, Kay E, Bouchier-Hayes DJ. Cyclo-oxygenase inhibition reduces tumour growth and metastasis in an orthotopic model of breast cancer. Br J Cancer. 2002 Jul 15;87(2):231–237.

87. Rodrigues P, Bangali H, Hammoud A, Mustafa YF, Al-Hetty HRAK, Alkhafaji AT, Deorari MM, Al-Taee MM, Zabibah RS, Alsalamy A. COX 2-inhibitors; a thorough and updated survey into combinational therapies in cancers. Vol. 41, Medical Oncology. Springer; 2024.

88. Perroud HA, Alasino CM, Rico MJ, Mainetti LE, Queralt F, Pezzotto SM, Rozados VR, Graciela Scharovsky O. Metastatic breast cancer patients treated with low-dose metronomic chemotherapy with cyclophosphamide and celecoxib: Clinical outcomes and biomarkers of response. Cancer Chemother Pharmacol. 2016 Feb 1;77(2):365–374.

89. Sung MW, Lee DY, Park SW, Oh SM, Choi JJ, Shin ES, Kwon SK, Ahn SH, Kim YH. Celecoxib enhances the inhibitory effect of 5-FU on human squamous cell carcinoma proliferation by ROS production. Laryngoscope. 2017 Apr 1;127(4):E117–123.

90. Chu TH, Chan HH, Hu TH, Wang EM, Ma YL, Huang SC, Wu JC, Chang YC, Weng WT, Wen ZH, Wu DC, Chen YMA, Tai MH. Celecoxib enhances the therapeutic efficacy of epirubicin for Novikoff hepatoma in rats. Cancer Med. 2018 Jun 1;7(6):2567–8250.

91. Singh S. Liposome encapsulation of doxorubicin and celecoxib in combination inhibits progression of human skin cancer cells. Int J Nanomedicine. 2018;13:11–23.

92. Cao Y, Qu J, Li C, Yang D, Hou K, Zheng H, Liu Y, Qu X. Celecoxib sensitizes gastric cancer to rapamycin via inhibition of the Cbl-b-regulated PI3K/Akt pathway. Tumor Biology. 2015 Jul 29;36(7):5607–5615.

93. Zhang T, Liu H, Li Y, Li C, Wan G, Chen B, Li C, Wang Y. A pH-sensitive nanotherapeutic system based on a marine sulfated polysaccharide for the treatment of metastatic breast cancer through combining chemotherapy and COX-2 inhibition. Acta Biomater. 2019 Nov 1;99:412–425.

94. Abdallah FM, Helmy MW, Katary MA, Ghoneim AI. Synergistic antiproliferative effects of curcumin and celecoxib in hepatocellular carcinoma HepG2 cells. Naunyn Schmiedebergs Arch Pharmacol. 2018;391:1399–1410.

95. Yang CX, Xing L, Chang X, Zhou TJ, Bi YY, Yu ZQ, Zhang ZQ, Jiang HL. Synergistic Platinum(II) Prodrug Nanoparticles for Enhanced Breast Cancer Therapy. Mol Pharm. 2020 Apr 6;17(4):1300–9. Available from: https://doi.org/10.1021/acs.molpharmaceut.9b01318

96. Sun J, Liu NB, Zhuang HQ, Zhao LJ, Yuan ZY, Wang P. Celecoxib-erlotinib combination treatment enhances radiosensitivity in A549 human lung cancer cell. Cancer Biomarkers. 2017;19:45–50.

97. Li N, Li H, Su F, Li J, Ma X, Gong P. Relationship between epidermal growth factor receptor (EGFR) mutation and serum cyclooxygenase-2 Level, and the synergistic effect of celecoxib and gefitinib on EGFR expression in non-small cell lung cancer cells. Vol. 8, Int J Clin Exp Pathol. 2015. Available from: www.ijcep.com/

98. Lin JZ, Hameed I, Xu Z, Yu Y, Ren ZY, Zhu JG. Efficacy of gefitinib-celecoxib combination therapy in docetaxel-resistant prostate cancer. Oncol Rep. 2018 Oct 1;40(4):2242–2250.

99. Hua H, Chen W, Shen L, Sheng Q, Teng L. Honokiol augments the anti-cancer effects of oxaliplatin in colon cancer cells. Acta Biochim Biophys Sin (Shanghai). 2013 Sep;45(9):773–779.

100. Zhao Q, Guo J, Wang G, Chu Y, Hu X. Suppression of immune regulatory cells with combined therapy of celecoxib and sunitinib in renal cell carcinoma. Vol. 8, Oncotarget. 2017. Available from: www.impactjournals.com/oncotarget/

101. Zhong J, Xiu P, Dong X, Wang F, Wei H, Wang X, Xu Z, Liu F, Li T, Wang Y, Li J. Meloxicam combined with sorafenib synergistically inhibits tumor growth of human hepatocellular carcinoma cells via ER stress-related apoptosis. Oncol Rep. 2015 Oct 1;34(4):2142–2150.

102. Li L, Zhong L, Tang C, Gan L, Mo T, Na J, He J, Huang Y. CD105: tumor diagnosis, prognostic marker and future tumor therapeutic target. Vol. 24, Clinical and Translational Oncology. Springer Science and Business Media Deutschland GmbH; 2022. p. 1447–1458.

103. Mohamed SY, Mohammed HL, Ibrahim HM, Mohamed EM, Salah M. Role of VEGF, CD105, and CD31 in the Prognosis of Colorectal Cancer Cases. J Gastrointest Cancer. 2019 Mar 15;50(1):23–34.

104. Ahluwalia MS, Rogers LR, Chaudhary R, Newton H, Ozair A, Khosla AA, Nixon AB, Adams BJ, Seon BK, Peereboom DM, Theuer CP. Endoglin inhibitor TRC105 with or without bevacizumab for bevacizumab-refractory glioblastoma (ENDOT): a multicenter phase II trial. Communications Medicine. 2023 Sep 8;3(1).

105. Thomas MJ, Major E, Benedek A, Horváth I, Máthé D, Bergmann R, Szász AM, Krenács T, Benyó Z. Suppression of metastatic melanoma growth in lung by modulated electro-hyperthermia monitored by a minimally invasive heat stress testing approach in mice. Cancers (Basel). 2020 Dec 1;12(12):1–24.

106. Thyagarajan A, Saylae J, Sahu RP. Acetylsalicylic acid inhibits the growth of melanoma tumors via SOX2-dependent-PAF-R-independent signaling pathway. 2017. Available from: www.impactjournals.com/oncotarget

107. Huang DW, Sherman BT, Tan Q, Kir J, Liu D, Bryant D, Guo Y, Stephens R, Baseler MW, Lane HC, Lempicki RA. DAVID Bioinformatics Resources: Expanded annotation database and novel algorithms to better extract biology from large gene lists. Nucleic Acids Res. 2007 Jul;35(SUPPL.2).

108. Bell CR, Pelly VS, Moeini A, Chiang SC, Flanagan E, Bromley CP, Clark C, Earnshaw CH, Koufaki MA, Bonavita E, Zelenay S. Chemotherapy-induced COX-2 upregulation by cancer cells defines their inflammatory properties and limits the efficacy of chemoimmunotherapy combinations. Nat Commun. 2022 Dec 1;13(1).

109. Ferrario A, Fisher AM, Rucker N, Gomer CJ. Celecoxib and NS-398 enhance photodynamic therapy by increasing in vitro apoptosis and decreasing in vivo inflammatory and angiogenic factors. Cancer Res. 2005 Oct 15;65(20):9473–9478.

110. Bokhari SMZ, Aloss K, Leroy Viana PH, Schvarcz CA, Besztercei B, Giunashvili N, Bócsi D, Koós Z, Balogh A, Benyó Z, Hamar P. Digoxin-Mediated Inhibition of Potential Hypoxia-Related Angiogenic Repair in Modulated Electro-Hyperthermia (mEHT)-Treated Murine Triple-Negative Breast Cancer Model. ACS Pharmacol Transl Sci. 2024 Jan 9; Available from: https://pubs.acs.org/doi/10.1021/acsptsci.3c00296

111. Mokhtari RB, Homayouni TS, Baluch N, Morgatskaya E, Kumar S, Das B, Yeger H. Combination therapy in combating cancer SYSTEMATIC REVIEW: COMBINATION THERAPY IN COMBATING CANCER BACKGROUND. Vol. 8. 2017. Available from: www.impactjournals.com/oncotarget

112. NHS England. Widespread clinical support for reforming NHS cancer standards to speed up diagnosis for patients. 2023.

113. Xie B, Stammes MA, Van Driel PBAA, Cruz LJ, Knol-Blankevoort VT, Löwik MAM, Mezzanotte L, Que I, Chan A, Van Den Wijngaard JPHM, Siebes M, Gottschalk S, Razansky D, Ntziachristos V, Keereweer S, Horobin RW, Hoehn M, Kaijzel EL, Van Beek ER, Snoeks TJA, Löwik CWGM. Necrosis avid near infrared fluorescent cyanines for imaging cell death and their use to monitor therapeutic efficacy in mouse tumor models. Vol. 6. Available from: www.impactjournals.com/oncotarget

114. Wolf BB, Schuler M, Echeverri F, Green DR. Caspase-3 is the primary activator of apoptotic DNA fragmentation via DNA fragmentation factor-45/inhibitor of caspase-activated DNase inactivation. Journal of Biological Chemistry. 1999 Oct 22;274(43):30651–30656.

115. Pfeffer CM, Singh ATK. Apoptosis: A target for anticancer therapy. Vol. 19, International Journal of Molecular Sciences. MDPI AG; 2018.

116. Carneiro BA, El-Deiry WS. Targeting apoptosis in cancer therapy. Vol. 17, Nature Reviews Clinical Oncology. Nature Research; 2020. p. 395–417.

117. Connolly EM, Harmey JH, O'Grady T, Foley D, Roche-Nagle G, Kay E, Bouchier-Hayes DJ. Cyclo-oxygenase inhibition reduces tumour growth and metastasis in an orthotopic model of breast cancer. Br J Cancer. 2002 Jul 15;87(2):231–237.

118. Min Zhou X, Chun Yu Wong B, Ming Fan X, Bo Zhang H, Chia Mi Lin M, Fu Kung H, Ming Fan D, Kum Lam S. Non-steroidal anti-inflammatory drugs induce apoptosis in gastric cancer cells through up-regulation of bax and bak. Vol. 22, Carcinogenesis. 2001.

119. Kuo IM, Lee JJ, Wang YS, Chiang HC, Huang CC, Hsieh PJ, Han W, Ke CH, Liao ATC, Lin CS. Potential enhancement of host immunity and anti-tumor efficacy of nanoscale curcumin and resveratrol in colorectal cancers by modulated electro-hyperthermia. BMC Cancer. 2020 Jun 29;20(1).

120. Nair A, Jacob S. A simple practice guide for dose conversion between animals and human. J Basic Clin Pharm. 2016;7(2):27.

121. Fanaroff AC, Roe MT. Contemporary Reflections on the Safety of Long-Term Aspirin Treatment for the Secondary Prevention of Cardiovascular Disease. Vol. 39, Drug Safety. Springer International Publishing; 2016. p. 715–727.

122. Shin S. Safety of celecoxib versus traditional nonsteroidal anti-inflammatory drugs in older patients with arthritis. J Pain Res. 2018;11:3211–3219.

123. Aloss K, Bokhari SMZ, Leroy Viana PH, Giunashvili N, Schvarcz CA, Szénási G, Bócsi D, Koós Z, Storm G, Miklós Z, Benyó Z, Hamar P. Modulated Electro-Hyperthermia Accelerates Tumor Delivery and Improves Anticancer Activity of Doxorubicin Encapsulated in Lyso-Thermosensitive Liposomes in 4T1-Tumor-Bearing Mice. Int J Mol Sci. 2024 Mar 7;25(6):3101. Available from: https://www.mdpi.com/1422-0067/25/6/3101

124. Lu P, Takai K, Weaver VM, Werb Z. Extracellular Matrix degradation and remodeling in development and disease. Cold Spring Harb Perspect Biol. 2011 Dec;3(12).

125. Cal S, López-Otín C. ADAMTS proteases and cancer. Vols. 44–46, Matrix Biology. Elsevier; 2015. p. 77–85.

126. Bonnans C, Chou J, Werb Z. Remodelling the extracellular matrix in development and disease. Vol. 15, Nature Reviews Molecular Cell Biology. Nature Publishing Group; 2014. p. 786–801.

127. Kelwick R, Wagstaff L, Decock J, Roghi C, Cooley LS, Robinson SD, Arnold H, Gavrilovic J, Jaworski DM, Yamamoto K, Nagase H, Seubert B, Krüger A, Edwards DR. Metalloproteinase-Dependent and -Independent processes contribute to inhibition of breast cancer cell migration, angiogenesis and liver metastasis by a disintegrin and metalloproteinase with thrombospondin motifs-15. Int J Cancer. 2015 Feb 15;136(4):E14–26.

128. Binder MJ, McCoombe S, Williams ED, McCulloch DR, Ward AC. ADAMTS-15 has a tumor suppressor role in prostate cancer. Biomolecules. 2020 May 1;10(5).

129. Porter S, Span PN, Sweep FCGJ, Tjan-Heijnen VCG, Pennington CJ, Pedersen TX, Johnsen M, Lund LR, Rømer J, Edwards DR. ADAMTS8 and ADAMTS15 expression predicts survival in human breast carcinoma. Int J Cancer. 2006 Mar 1;118(5):1241–1247.

130. Kelwick R, Wagstaff L, Decock J, Roghi C, Cooley LS, Robinson SD, Arnold H, Gavrilovic J, Jaworski DM, Yamamoto K, Nagase H, Seubert B, Krüger A, Edwards DR. Metalloproteinase-Dependent and -Independent processes contribute to inhibition of breast cancer cell migration, angiogenesis and liver metastasis by a disintegrin and metalloproteinase with thrombospondin motifs-15. Int J Cancer. 2015 Feb 15;136(4):E14–26.

131. Liang L, Zhu JH, Chen G, Qin XG, Chen JQ. Prognostic Values for the mRNA Expression of the ADAMTS Family of Genes in Gastric Cancer. J Oncol. 2020;2020.

132. Cangemi C, Hansen ML, Argraves WS, Rasmussen LM. Fibulins and Their Role in Cardiovascular Biology and Disease. Adv Clin Chem. 2014 Jan 1;67:245–265.

133. Zhu XJ, Liu J, Xu XY, Zhang CD, Dai DQ. Novel tumor-suppressor gene epidermal growth factor-containing fibulin-like extracellular matrix protein 1 is epigenetically silenced and associated with invasion and metastasis in human gastric cancer. Mol Med Rep. 2014;9(6):2283–2292.

134. Kaur J, Reinhardt DP. Extracellular Matrix (ECM) Molecules. Stem Cell Biology and Tissue Engineering in Dental Sciences. 2015 Jan 1;25–45.

135. Sadr-Nabavi A, Ramser J, Volkmann J, Naehrig J, Wiesmann F, Betz B, Hellebrand H, Engert S, Seitz S, Kreutzfeld R, Sasaki T, Arnold N, Schmutzler R, Kiechle M, Niederacher D, Harbeck N, Dahl E, Meindl A. Decreased expression of angiogenesis antagonist EFEMP1 in sporadic breast cancer is caused by aberrant promoter methylation and points to an impact of EFEMP1 as molecular biomarker. Int J Cancer. 2009 Apr 1;124(7):1727–1735.

136. Albig AR, Neil JR, Schiemann WP. Fibulins 3 and 5 antagonize tumor angiogenesis in vivo. Cancer Res. 2006 Mar 1;66(5):2621–2629.

137. Fararjeh AS, Kaddumi E, Khader A Al, Aloliqi AA. The Diagnostic and Prognostic Significance of EFEMP1 in Breast Cancer: An Immunohistochemistry Study. Int J Surg Pathol. 2023;31(6):1057–1066. Available from: https://doi.org/10.1177/10668969221126122

138. Zhang X, Wu J, Hu C, Zheng X, Guo Z, Li L. CXCL11 negatively regulated by MED19 favours antitumour immune infiltration in breast cancer. Cytokine. 2023 Feb 1;162.

139. Li F, Zhang H, Wang Y, Yao Z, Xie K, Mo Q, Fan Q, Hou L, Deng F, Tan W. FGFBP1 as a potential biomarker predicting bacillus Calmette–Guérin response in bladder cancer. Front Immunol. 2022 Sep 2;13.

140. Czubayko· F, Liaudet-Coopman° EDE, Aigner A, Tuveson AT, Berchem G], Wellsteln A. A secreted FGF-binding protein can serve as the angiogenic switch in human cancer. 1997. Available from: http://www.nature.com/naturemedicine

141. Chang ACM, Doherty J, Huschtscha LI, Redvers R, Restall C, Reddel RR, Anderson RL. STC1 expression is associated with tumor growth and metastasis in breast cancer. Clin Exp Metastasis. 2015 Jan 28;32(1):15–27.

142. Chen F, Zhang Z, Pu F. Role of stanniocalcin-1 in breast cancer (Review). Vol. 18, Oncology Letters. Spandidos Publications; 2019. p. 3946–3953.

143. Pemmari A, Tuure L, Hämäläinen M, Leppänen T, Moilanen T, Moilanen E. Effects of ibuprofen on gene expression in chondrocytes from patients with osteoarthritis as determined by RNA-Seq. RMD Open. 2021 Sep 8;7(3).

144. Magnussen SN, Toraskar J, Wilhelm I, Hasko J, Figenschau SL, Molnar J, Seppola M, Steigen SE, Steigedal TS, Hadler-Olsen E, Krizbai IA, Svineng G. Nephronectin promotes breast cancer brain metastatic colonization via its integrin-binding domains. Sci Rep. 2020 Dec 1;10(1).

145. van Kooyk Y, Ilarregui JM, van Vliet SJ. Novel insights into the immunomodulatory role of the dendritic cell and macrophage-expressed C-type lectin MGL. Immunobiology. 2015;220(2):185–192.

146. Shaoqing LIU, Zhang J, Jiujun ZHU, Jiao D, Zhenzhen LIU. Prognostic values of EDNRB in triple-negative breast cancer. Oncol Lett. 2020 Aug 1;20(5).

147. Jenkins BD, Martini RN, Hire R, Brown A, Bennett B, Brown I, Howerth EW, Egan M, Hodgson J, Yates C, Kittles R, Chitale D, Ali H, Nathanson D, Nikolinakos P, Newman L, Monteil M, Davis MB. Atypical chemokine receptor 1 (DARC/ACKR1) in breast tumors is associated with survival, circulating chemokines, tumor-infiltrating immune cells, and African ancestry. Cancer Epidemiology Biomarkers and Prevention. 2019 Apr 1;28(4):690–700.

148. Peppino G, Ruiu R, Arigoni M, Riccardo F, Iacoviello A, Barutello G, Quaglino E. Teneurins: Role in cancer and potential role as diagnostic biomarkers and targets for therapy. Vol. 22, International Journal of Molecular Sciences. MDPI AG; 2021. p. 1–23.

149. Zhang R, Jiang HX, Liu YJ, He GQ. Structure, function, and pathology of Neurexin-3. Vol. 10, Genes and Diseases. KeAi Communications Co.; 2023. p. 1908–1919.

150. Hanahan D, Monje M. Cancer hallmarks intersect with neuroscience in the tumor microenvironment. Vol. 41, Cancer Cell. Cell Press; 2023. p. 573–580.

151. Dai D, Liu H. The Nervous System Contributes to the Tumorigenesis and Progression of Human Digestive Tract Cancer. Vol. 2022, Journal of Immunology Research. Hindawi Limited; 2022.

152. Kusinska R, Goírniak P, Pastorczak A, Fendler W, Potemski P, Mlynarski W, Kordek R. Influence of genomic variation in FTO at 16q12.2, MC4R at 18q22 and NRXN3 at 14q31 genes on breast cancer risk. Mol Biol Rep. 2012 Mar;39(3):2915–2919.

153. Fox BP, Kandpal RP. EphB6 receptor significantly alters invasiveness and other phenotypic characteristics of human breast carcinoma cells. Oncogene. 2009 Apr 9;28(14):1706–1713.

154. Osta WA, Chen Y, Mikhitarian K, Mitas M, Salem M, Hannun YA, Cole DJ, Gillanders WE. EpCAM Is Overexpressed in Breast Cancer and Is a Potential Target for Breast Cancer Gene Therapy. Vol. 64, CANCER RESEARCH. 2004. Available from: www.mpibpc.gwdg.de/abteilungen/100/105/sirna.html.

155. Gao S, Sun Y, Liu X, Zhang D, Yang X. EpCAM and COX-2 expression are positively correlated in human breast cancer. Mol Med Rep. 2017 Jun 1;15(6):3755–3760.

10.Bibliography of the candidate's publications

I. Publications used in the thesis

Giunashvili N, Thomas JM, Schvarcz CA, Viana PHL, Aloss K, Bokhari SMZ, Koós Z, Bócsi D, Major E, Balogh A, Benyó Z, Hamar P. Enhancing therapeutic efficacy in triple-negative breast cancer and melanoma: synergistic effects of modulated electro-hyperthermia (mEHT) with NSAIDs especially COX-2 inhibition in in vivo models. Mol Oncol. 2024 Jan 12. doi: 10.1002/1878-0261.13585. Epub ahead of print. PMID: 38217262. **IF: 6.6**

Bokhari SMZ, Aloss K, Leroy Viana PH, Schvarcz CA, Besztercei B, **Giunashvili N**, Bócsi D, Koós Z, Balogh A, Benyó Z, Hamar P. Digoxin-Mediated Inhibition of Potential Hypoxia-Related Angiogenic Repair in Modulated Electro-Hyperthermia (mEHT)-Treated Murine Triple-Negative Breast Cancer Model. ACS Pharmacol Transl Sci. 2024 Jan 9;7(2):456-466. doi: 10.1021/acsptsci.3c00296. PMID: 38357275; PMCID: PMC10863435. **IF:6.0**

ii. Publications, related to but not included in the thesis

Aloss, K.; Bokhari, S.M.Z.; Leroy Viana, P.H.; **Giunashvili, N**.; Schvarcz, C.A.; Szénási, G.; Bócsi, D.; Koós, Z.; Storm, G.; Miklós, Z.; et al. Modulated Electro-Hyperthermia Accelerates Tumor Delivery and Improves Anticancer Activity of Doxorubicin Encapsulated in Lyso-Thermosensitive Liposomes in 4T1-Tumor-Bearing Mice. *Int. J. Mol. Sci.* 2024, *25*, 3101. https://doi.org/10.3390/ijms25063101 IF:6.2

Viana PHL, Schvarcz CA, Danics LO, Besztercei B, Aloss K, Bokhari SMZ, **Giunashvili N**, Bócsi D, Koós Z, Benyó Z, Hamar P. Heat shock factor 1 inhibition enhances the effects of modulated electro hyperthermia in a triple negative breast cancer mouse model. Sci Rep. 2024 Apr 8;14(1):8241. doi: 10.1038/s41598-024-57659-x. PMID: 38589452; PMCID: PMC11002009. IF:4.6

11.Acknowledgments

First, I would like to express my gratitude to my supervisor, Professor Péter Hamar for his guidance, support, and encouragement throughout my PhD journey.

I would also like to extend my heartful thanks to the members of my thesis committee: Professor Oláh- Német Orsolya and Professor Szentmártoni Gyöngyvér for their constructive criticism and helpful suggestions that significantly improved the quality of my research.

I am grateful to my internal defense reviewer Tamás Vancsik, PhD for his deep reading and criticism and for encouraging me during my PhD journey.

I am incredibly grateful to my colleagues and friends at Semmelweis University for their help and enriching my research experience: Head of the doctoral school, Professor Zoltan Benyó for all his support. My colleagues - Jeremiah Mbuotidem Thomas, Csaba András Schvarcz, Pedro Henrique Leroy Viana, Kenan Aloss, Syeda Mahak Zahra Bokhari, Zoltán Koós, Daniel Bocsi, Tamás Vancsik, Lea Danics, Enikő Major, Andrea Balogh.

A special mention goes to my family, to my parents and sisters. I am incredibly grateful to my grandparents for their endless love and support. I thank all for their constant encouragement and for being a source of strength.

Finally, to my friends, both near and far, thank you for your unwavering support, and understanding, and for always being there to lift my spirits.

This thesis is dedicated to all those who believed in me and provided the support needed to reach this milestone. Thank you all from the bottom of my heart.